Essential roles of ECAT15-2/Dppa2 in functional lung development.

AUTHOR(S):

Nakamura, Tomonori; Nakagawa, Masato; Ichisaka, Tomoko; Shiota, Arufumi; Yamanaka, Shinya

CITATION:

Nakamura, Tomonori ...[et al]. Essential roles of ECAT15-2/Dppa2 in functional lung development.. Molecular and cellular biology 2011, 31(21): 4366-4378

ISSUE DATE:

2011-11

URL:

http://hdl.handle.net/2433/152301

Essential roles of ECAT15-2/Dppa2 in functional lung development

Tomonori Nakamura(1), Masato Nakagawa(1,2), Tomoko Ichisaka(1,4), Arufumi Shiota(1) and Shinya Yamanaka*(1-4)

1) Center for iPS Cell Research and Application (CiRA), Kyoto University, Kyoto 606-8507, Japan

2) Yamanaka iPS Cell Special Project, Japan Science and Technology Agency, Kawaguchi 332-0012, Japan.

3) Gladstone Institute of Cardiovascular Disease, San Francisco, CA 94158, USA

4) Institute for Integrated Cell-Material Sciences (iCeMS), Kyoto University, Kyoto 606-8507, Japan

Correspondence: yamanaka@cira.kyoto-u.ac.jp

Phone; +81-75-366-7044

FAX; +81-75-366-7042

Running title; ECAT15-2 regulates genes expressed in future.

Material and methods; 1,007 words

Introduction, Results and Discussion; 4,634 words

<Summary>

Many transcription factors and DNA binding proteins play essential roles in the development of organs in which they are highly and/or specifically expressed. *Embryonic stem cell (ESC) associated transcript (ECAT) 15-1* and *ECAT15-2*, also known as *developmental pluripotency-associated (Dppa) 4* and *Dppa2*, are enriched in mouse ESCs and pre-implantation embryos, and encode homologous proteins with a common DNA binding domain known as the SAP motif. Previously, ECAT15-1 was shown to be important in the lung development, while it is dispensable in early development. In this study, we generated ECAT15-2 single and ECAT15-1/15-2 double knockout mice and found that almost all mutants, like ECAT15-1 mutants, died around birth with respiratory defects. Paradoxically, the expression of neither ECAT15-1 nor ECAT15-2 was detected in lung organogenesis. Several genes, such as Nkx2-5, Gata4, and Pitx2 were down-regulated in the *ECAT15-2*-null lung. On the other hand, genomic DNA of these genes showed inactive chromatin statuses in ECAT15-2-null ESCs, but not in wild-type ESCs. Chromatin immuno-precipitation (ChIP) assay revealed that ECAT15-2 binds to the regulatory region of *Nkx2-5* in ESCs. These data suggest that ECAT15-2 have important roles in lung development where it is no longer expressed, by leaving epigenetic marks from earlier developmental stages.

<Introduction>

ECAT15-1 and *ECAT15-2* are members of *ES cell associated transcripts (ECATs)*, which were identified as genes enriched in mouse ESCs by *in silico* differential display screening **(18)**. The two genes were also known as *Dppa (developmental pluripotency-associated) 4* and *Dppa2*, which were identified as novel markers of undifferentiated mouse ESCs with expression patterns similar to Oct3/4 **(3)**.

ECAT15-1 and *ECAT15-2* are tandemly located on the 16th chromosome in the mouse genome and have similar exon-intron structures, encoding polypeptides with 32% identity at the amino acid sequences **(13)**. They contain a common putative DNA binding domain, SAP motif, which consists of two amphipathic helices separated by an invariant glycine, and have DNA/RNA binding ability and function in chromatin modification **(1)**. ECAT15-1 and ECAT15-2 show a weak homology to another SAP-domain containing protein, PGC7/stella/Dppa3 **(3)**, which binds DNA and protects the maternal genome from global demethylation in fertilized eggs **(19)**. Therefore, ECAT15-1 and ECAT15-2 may regulate gene expressions through modifying the epigenetic status, like Dppa3. Indeed, ECAT15-1 has been shown to associate with chromatin and may therefore play a role in transcriptionally active regions **(16)**.

The specific expressions suggest that the two genes play roles in pluripotency and early mouse development. However, ECAT15-1 single and ECAT15-1/15-2 double mutant ESCs showed no significant phenotypes **(11)**. Furthermore, ECAT15-1 deletion in mice did not affect the early

52 embryogenesis. Thus, ECAT15-1 and ECAT15-2 are apparently dispensable in early mouse
53 development and derivation and maintenance of ESCs regardless their specific expressions.

54 Unexpectedly, ECAT15-1 single mutant mice showed perinatal lethality, with deficiency in
55 lung alveolar formation and rib abnormalities. **(11)**. Paradoxically, the authors were unable to detect
56 the expression of ECAT15-1 in these organs in wild-type mice by RT-PCR. **(11)**. Thus, it remains
57 elusive how ECAT15-1 contributes to functional organogenesis where it is no longer expressed.
58 Functions of ECAT15-2 *in vivo* also remained to be determined.

59 In order to further clarify the functions of ECAT15-1 and ECAT15-2, as well as the
60 relationship of the two related proteins, we generated mutant mice deficient in ECAT15-1,
61 ECAT15-2, or both. Since *ECAT15-1* and *ECAT15-2* are tandemly located on the same chromosome,
62 we established an ECAT15-1/15-2 double conditional targeting system using bacterial artificial
63 chromosome (BAC).

<Result>

Generation of ECAT15-1/15-2 single and double heterozygous mutant mice using double conditional BAC vector

We generated ECAT15-1 single, ECAT15-2 single and ECAT15-1/15-2 double mutant mice in order to investigate the functions and relationships between ECAT15-1 and ECAT15-2 *in vivo*. It would be difficult to generate ECAT15-1/15-2 double mutant mice by mating single mutant mice of each allele because the two genes are located on the same chromosome and are separated by only ~17 kbps **(13)**. Therefore, we constructed an ECAT15-1/15-2 double conditional targeting vector using BAC **(Figure 1A)**. This BAC vector has three loxP sites and a pgk-neomycin resistant gene cassette in the *ECAT15-1* locus, and three FRT sites and a pgk-Hygromycin resistant gene cassette in the *ECAT15-2* locus. The vector was introduced into RF8 ESCs **(18)** by electroporation and the cells were selected using both G418 and hygromycin. Southern blot analyses with an external probe (ECAT15_3' probe) showed that two clones (CT#28 and CT#31), out of 48 screened, possessed bands corresponding to the correctly targeted alleles (CT allele, Conditional Targeting allele) at both *ECAT15-1* and *ECAT15-2* **(Figure 1B and Supplementary Figure 1B & C)**. Real-time PCR with Taqman probes showed that these two clones have only one copy of the wild-type alleles of *ECAT15-1* and *ECAT15-2*, further confirming the homologous recombination **(Figure 1C)**. Southern blot analyses with an internal probe (Hyg probe) did not detect extra bands, indicating that these clones are free random integrations of the BAC targeting vector **(Figure 1B and Supplementary**

Figure 1B & C). These ESCs were injected into blastocysts to generate 15-1$^{+/CT}$, 15-2$^{+/CT}$ mice and subsequently 15-1$^{CT/CT}$, 15-2$^{CT/CT}$ mice **(Supplementary Figure 1A)**, which were normal in gross appearance and fertile. Therefore, the conditional alleles do not disturb the development of somatic organs and germ cells.

ECAT15-1 and/or ECAT15-2 were singly or doubly deleted by mating the 15-1$^{+/CT}$, 15-2$^{+/CT}$ mice with EIIA-Cre transgenic mice **(10)** and Rosa26-FLPe transgenic mice **(5) (Figure 1D)**. To disrupt ECAT15-1, the 15-1$^{+/-}$, 15-2$^{+/CT}$ mice were generated by mating the 15-1$^{+/CT}$, 15-2$^{+/CT}$ mice with EIIA-Cre mice. Then the 15-1$^{+/-}$, 15-2$^{+/CT}$ mice were mated with Rosa26-FLPe transgenic mice to obtain the 15-1$^{+/-}$, 15-2$^{+/FRT}$ mice **(Supplementary Figure 2A)**. To delete ECAT15-2, the 15-1$^{+/CT}$, 15-2$^{+/-}$ mice were generated by mating the 15-1$^{+/CT}$, 15-2$^{+/CT}$ mice with Rosa26-FLPe mice. Then the 15-1$^{+/CT}$, 15-2$^{+/-}$ mice were mated with EIIA-Cre mice to obtain the 15-1$^{+/Flox}$, 15-2$^{+/-}$ mice **(Supplementary Figure 2B).** The ECAT15-1/15-2 double heterozygous mutant (15-1$^{+/-}$, 15-2$^{+/-}$) mice were generated from the mating of the 15-1$^{+/-}$, 15-2$^{+/CT}$ mice and Rosa26-FLPe mice **(Supplementary Figure 2C).**

Although there were no obvious abnormalities in the 15-1$^{CT/CT}$, 15-2$^{CT/CT}$ mice, the residual loxP and FRT sites may affect the expression of ECAT15-1 or ECAT15-2. Thus, we selected single heterozygous mutant mice in which these cassettes had been removed by Cre or FLPe-mediated recombination (the 15-1$^{+/-}$, 15-2$^{+/FRT}$ mice and the 15-1$^{+/Flox}$, 15-2$^{+/-}$ mice). Nevertheless qRT-PCR analysis detected abnormal expression from the 15-2FRT allele in testis (more than 1000-fold

increase in comparison to wild-type) (**Supplementary Figure 2D& E**). However, the ECAT15-2 protein was not detected by Western blotting in the testis of the 15-1$^{+/-}$, 15-2$^{+/FRT}$ mice **(Supplementary Figure. 2F)**. The aberrant ECAT15-2 transcript was not detected in other organs or tissues examined. All three types of heterozygous mutant mice were normal in gross appearance and fertile. Therefore we concluded that the aberrant ECAT15-2 transcript did not disturb normal development.

Analyses of ECAT15 single and double homozygous mutant mice

Heterointercross analysis using each of the ECAT15 heterozygous mutant mice was performed. The 15-1$^{+/-}$, 15-2$^{+/FRT}$ intercross generated slightly smaller number of the 15-1KO (15-1$^{-/-}$, 15-2$^{FRT/FRT}$) embryos than that expected from Mendelian law at E18.5 **(Table 1A)**. The mortality of the 15-1KO pups was increasing at birth **(Table 1A)**, and most of the 15-1KO neonates died within 3 days **(Supplementary Figure 3A)** and around weaning age (~five weeks old), we found that only 14 of 423 (3.3%) were the 15-1KO **(Table 1A)**. The few surviving 15-1KO neonates showed growth retardation **(Supplementary Figure 3B)**, but they caught up with wild-type and the 15-1$^{+/-}$, 15-2$^{+/FRT}$ mice by twenty weeks of age **(Supplementary Figure 3C)**. These results indicated that ECAT15-1 is dispensable for peri-implantation development, but is important for the growth and survival during neonatal period.

Next, the 15-1$^{+/Flox}$ 15-2$^{+/-}$ mice were intercrossed to study the functions of ECAT15-2. The

15-2 homozygous mutant (15-2KO, 15-1$^{Flox/Flox}$, 15-2$^{-/-}$) embryos were identified in accordance with the Mendelian ratio by E16.5. However at E18.5 and P0, the number of the 15-2KO embryos were fewer than expected, started to show the mortality **(Table 1B)**. None of these 15-2KO neonates survived by weaning age **(Table 1B).** These data indicated that ECAT15-2 is dispensable for the peri-implantation embryo, but play important roles during late embryogenesis and is essential for the survival of neonates.

Finally, the 15-1$^{+/-}$, 15-2$^{+/-}$ mice were intercrossed to determine whether ECAT15-1 and ECAT15-2 function complementary in early embryogenesis, where both proteins are expressed. Unexpectedly, at E18.5, the DoubleKO embryos (15-1$^{-/-}$, 15-2$^{-/-}$) were found in accordance with Menderian ratio **(Table 1C)**. The DoubleKO neonates showed small birth weight **(Supplementary Figure 3D)** and its number was also appeared significantly small compared to that of sibs **(Table 1C)**. In weaning age, the DoubleKO mice were found only 13 out of 451 (2.9%) **(Table 1C)**. These data suggested that both ECAT15-1 and ECAT15-2 are dispensable for early embryogenesis, however they are important for survival of peri-natal stage. Interestingly, the deletion of both ECAT15-1 and ECAT15-2 resulted in a phenotype less severe than that of the 15-2KO **(Table 1A,B &C)**.

Next, we examined whether ECAT15-1 and ECAT15-2 play roles in normal fertility, since they are expressed in gonads **(13)**. We bred the 15-1KO mice and the DoubleKO mice which were more than eight weeks age with wild-type ones for a long period (more than five months). Both the male and female 15-1KO mice gave a birth several times (data not shown). Furthermore, the

DoubleKO male and female mice were also fertile; they also gave a birth several times (data not shown). It was not possible to perform sufficient mating to detect minor abnormalities related to fertility, since most of the 15-1KO or the DoubleKO mice died prior to maturation. Nevertheless, these facts showed that the functional germ cells are generated in the absence of ECAT15-1 or both ECAT15-1 and ECAT15-2.

Respiratory defects in ECAT15-1/15-2 single, double mutant embryo.

Further analyses were performed to make clear the reason why the three types of ECAT15 mutants die around birth. In the previous report, the ECAT15-1 mutant mice had respiratory defects **(11)**. This suggested that the 15-2KO mice and the DoubleKO mice also have breathing abnormalities. E18.5 embryos were collected from the 15-$1^{+/CT}$, 15-$2^{+/-}$ intercrosses by caesarian section. Six of 50 neonates rapidly became cyanotic and died within two hours (data not shown). Five of the six dead neonates were found to be the 15-2KO (15-$1^{CT/CT}$, 15-$2^{-/-}$). Whereas the lungs from surviving mice floated in water, the lungs from dead mice did not, thus indicating respiratory failure (data not shown).

Histological analyses of the lungs from the 15-1KO, the 15-2KO and the DoubleKO of E18.5 embryos revealed that 15-1KO lungs were similar to wild-type except for their slightly thicker mesenchyme than wild-type lungs **(Figure 2A)**. The 15-2KO lungs also showed thicker mesenchyme. In addition, they showed smaller alveolar spaces; their defects were apparently severer than those of

157 the 15-1KO lungs **(Figure 2A)**. The DoubleKO lungs also showed thicker mesenchyme and smaller
158 alveolar spaces, but the severity was more diverse than those of the 15-1KOs and 15-2KOs **(Figure**
159 **2A)**. At E16.5, in contrast, no clear differences were observed between wild-type lung and the
160 15-2KO mutants **(Supplementary Figure 4)**. Thus, the ECAT15 KO lungs have a morphologically
161 normal proximal epithelium, but an impaired alveolar architecture, and the lung deformities appear
162 mainly during the saccular stage, which starts from ~E17.5 in mouse development **(25)**.

163 Next, the expression pattern of lung airway epithelium markers was assessed by qRT-PCR
164 and immunohistochemistry. Scgb1a1 (secretoglobin, family 1A, member 1) is expressed in proximal
165 lung epithelium **(24)**, and SP-C (surfactant protein type C) is specific for alveolar cell type2 and
166 serves as a distal epithelium marker **(6)**. The 15-2KO lungs (E18.5) expressed significantly low
167 amount of Scgb1a1, and the 15-1KO and the DoubleKO lungs also expressed slightly less amount of
168 Scgb1a1 **(Figure 2B)**, despite the morphology of epithelial cells is normal **(Figure 2C)**. The lungs of
169 three types of ECAT15 KO lungs had normal SP-C expression levels **(Figure 2B)**, but SP-C positive
170 cells were buried in the mesenchyme **(**Arrows in **Figure 2C)**.

171 **ECAT15-1 and ECAT15-2 expression in lung development**

172 The abovementioned roles of ECAT15s lead to the expectation that they are expressed
173 during lung organogenesis. Lung and gonad RNA was prepared from C57/BL6 mouse embryos at
174 several developmental stages and analyzed by qRT-PCR. Both ECAT15-1 and ECAT15-2 transcripts

were detected in developing gonads at approximately ~10% of the level in undifferentiated ESCs **(Figure 3A)**. However, no expression of ECAT15s was detected in lungs **(Figure 3A)**.

To further address whether ECAT15s were expressed in specific cell populations such as somatic stem cells, the expression of ECAT15s was examined histologically either by *in situ* hybridization or by utilizing EGFP reporter mice. ECAT15-1 probes were generated for *in situ* hybridization and used to analyze serial axial-proximal axis sections of whole mouse embryos at E14.5. There were positive signals in the testis, but not in the lung **(Figure 3B)**. The 15-2-EGFP reporter mouse was generated to study the expression of ECAT15-2. The EGFP cDNA was introduced into the 1st exon of ECAT15-2 in the BAC clone and the reporter BAC was inserted into RF8 ESCs. The reporter ESCs showed strong EGFP signals when undifferentiated, but the signal rapidly decreased upon differentiation **(Supplementary Figure 5A)**. The reporter BAC was injected into fertilized eggs to generate the 15-2-EGFP reporter transgenic mice. The EGFP signals were detected in E3.5 blastocysts **(Supplementary Figure 5B)**. During later developmental period, the EGFP signal was detected only in the genital ridge of E14.5 embryos **(Figure 3C)**. No EGFP signals were detected in other organs or tissues, including the lung **(Figure 3C)**.

To further confirm the absence of ECAT15-2 expression in developing lung, we performed FACS analysis using dissociated cells isolated lung and testis of a 15-2-EGFP reporter embryo at E14.5. Approximately 1,000 EGFP positive cells were detected out of 50,000 cells derived from testis **(Figure 3D).** In great contrast, no EGFP positive cells were identified out of 500,000 cells from

lung **(Figure 3D)**. Taken together, these data demonstrated that neither ECAT15-1 nor ECAT15-2 is expressed during lung organogenesis.

Aberrant gene expression in ECAT15-2 mutant lungs

To identify molecular mechanisms of lung disorders in three types of the ECAT15 KO mice, the global gene expression pattern of the 15-2KO lungs was examined at E18.5, which showed the most severe phenotype with the smallest divergence among the three types of the ECAT15 KOs. Comparisons between three wild-type and three 15-2KO lungs revealed 106 entities that showed >2-fold expression changes **(Figure 4A, Supplementary Table 1A)**. Gene ontology analyses using the NEXTBIO program (www.nextbio.com) revealed significant enrichment of genes involved in contraction and muscle function among the 106 entities **(Supplementary Table 1B)**. These changes in global gene expression are consistent with the thicker mesenchyme detected in mutant lungs histologically.

The microarray analyses also detected aberrant expression of several development-related transcription factors, Gata4, Nkx2-5, Pitx1 and Pitx2 in the 15-2KO lungs **(Supplementary Table 1A)**. The expression of these genes among three types of the ECAT15 mutant lungs was examined by qRT-PCR **(Figure 4B)**. About all genes examined, the expression pattern in the 15-2KO lungs showed the biggest changes compared to wild-type among three types of the ECAT15 mutant lungs **(Figure 4B)**. There were also the aberrant expressions of Pitx2 in the 15-1KO lungs, and Pitx1 in

212 both the 15-1KO and the DoubleKO lungs **(Figure 4B)**. These data suggest that the abnormal
213 expression of these transcription factors may contribute to the impaired lung architecture found in the
214 three types of ECAT15 KO mice.

215 **Aberrant epigenetic status in ECAT15-2 mutant ESCs**

216 Due to the DNA binding domain, SAP motif, we hypothesized that ECAT15-1 and
217 ECAT15-2 affect lung development by modifying the epigenetic status of critical genes, such as the
218 four transcription factors **(Figure 4B)**, during earlier developmental stage when they are expressed.
219 To address this hypothesis, the 15-2KO ESCs were generated as an *in vitro* model of
220 pre-implantation embryos. The 15-2KO ($15\text{-}1^{CT/CT}$, $15\text{-}2^{-/-}$) ESCs were established from blastocysts
221 of heterozygous intercross mice **(Supplementary Figure 6A)**. The established 15-2KO ESCs
222 showed the morphology similar to their wild-type counterparts **(Supplementary Figure 6B)**, but
223 proliferated slightly slower than did the wild-type cells **(Supplementary Figure 6C)**. The 15-2KO
224 ESCs expressed pluripotency markers such as Oct3/4, Sox2 and Sall4 at levels comparable to those
225 in wild-type ESCs **(Supplementary Figure 6D)**. Thus, ECAT15-2 is dispensable in maintaining
226 pluripotency of mouse ESCs.

227 However, a comparison of global gene expression between wild-type and the 15-2KO
228 ESCs revealed that many genes were down-regulated in ECAT15-2KO ESCs **(Supplementary**
229 **Figure 6E)**. Of note, many of suppressed genes are involved in gonads and gametogenesis, such as

Ddx4, Mael, and *Syce1*. We also established rescue cells by expressing Flag-tagged ECAT15-2 in ECAT15-2KO ESCs by means of the *piggyBac* vector **(26) (Supplementary Figure 7A).** In the established cells, the expression level of ECAT15-2 was approximately 5-fold higher than that in wild-type ESCs **(Supplementary Figure 7B, C)**. Quantitative RT-PCR **(Supplementary Figure 7C)** and DNA microarray analyses **(Supplementary Figure 7D)** demonstrated that the altered gene expression observed in ECAT15-2 KO ESCs were reverted, albeit partially, by the forced expression of Flag-tagged ECAT15-2. The partial rescue may be attributable to the abnormally high expression levels of ECAT15-2. Nevertheless, these data demonstrated that ECAT15-2 is involved in the regulation of many genes in mouse ESCs.

We next analyzed epigenetic status in ECAT15-2KO ESCs. DNA methylation status was analyzed by bisulfate sequencing using genomic DNA of the 15-2KO ESCs, and we found that the promoter regions of *Syce1*, *Gata4*, and *Nkx2-5* were hyper-methylated in the 15-2KO ESCs **(Figure 5A)**. The promoter region of *Pitx2* in the 15-2KO ESCs was also methylated more than that of wild-type ESCs **(Figure 5A)**. Histone modification studies by ChIP assays revealed the enrichment of dimethylation at H3K9 in the *Nkx2-5* and *Syce1* promoter regions in the 15-2KO ESCs **(Figure 5B).** In contrast, histone trimethylation at H3K4 and H3K27 were normal in the mutant ESCs **(Supplementary Figure 8)**. To address whether these aberrant epigenetic status was regulated by ECAT15-2 directly, we also performed ChIP analyses using anti-ECAT15-2 antibody and found that ECAT15-2 binds to the promoters of *Nkx2-5* and *Syce1*, but not to that of *Gata4* **(Figure 5C).** These

data demonstrated that ECAT15-2 directly or indirectly maintains active DNA and histone modification status of the target genes in ESCs.

The epigenetic status was also examined in the 15-2KO lungs. Bisulfate genomic sequences showed that the promoter regions of tested five genes except *Syce1* in the 15-2KO lungs had a similar pattern of DNA methylation as the wild-type (**Figure 6A**). The promoter of *Syce1* had slightly methylated DNA pattern than the wild-type (**Figure 6A**). Similarly, ChIP analysis showed that histone dimethylation at H3K9 did not increase in the 15-2KO lungs in comparison to wild-type lungs (**Figure 6B**). Taken together, these data indicated that ECAT15-2 may affect gene expression in developing lung through the regulation of epigenetic status in early embryonic stage.

Analyses of molecular moieties of ECAT15s

Finally, to address the reasons why the 15-2KO mice showed more severe phenotypes than the DoubleKO mice did, molecular relationships between ECAT15-1 and ECAT15-2 were analyzed. The subcellular localization and protein-protein interactions of ECAT15-1 and ECAT15-2 were examined in the ESCs. Immunostaining with anti-ECAT15-1, anti-ECAT15-2 and anti-HP1α antibodies revealed that ECAT15-1 and ECAT15-2 were localized exclusively with HP1α in the nucleus **(Figure 7A)**. HP1α is known to localize in heterochromatin region **(2)**, thus the result suggests that both ECAT15-1 and ECAT15-2 are located at euchromatin regions. Immunoprecipitation with anti-ECAT15-2 antibody using lysates from wild-type and the 15-2KO

ESCs showed that ECAT15-1 and ECAT15-2 interact with each other **(Figure 7B)**. These data indicated that ECAT15-1 and ECAT15-2 form a complex and the balance of these genes may affect the gene expression and developmental process in lung.

<Discussion>

Our results demonstrated essential roles of ECAT15-1 and ECAT15-2 in functional lung development. Our result is consistent with the previous report that ECAT15-1 is important in normal lung function, indicating that the phenotypes we observed are attributable to loss of ECAT15 functions, but not to off target effects. Despite these important roles, we were unable to detect the expression of ECAT15s during lung organogenesis. In ESCs where ECAT15s are expressed, we found that ECAT15-1 and ECAT15-2 bind to target genes as a complex and maintain active epigenetic statues. We thus propose a model in which ECAT15 complex affects the expression of target genes at later developmental stages where ECAT15s are no longer expressed, by leaving epigenetic memories from earlier developmental stages.

How ECAT15s maintain active epigenetic statues, i.e. protecting DNA and histone H3K9 from hyper-methylation, in ESCs remains to be determined. We analyzed amino acid sequence of ECAT15-1 and ECAT15-2, and compared them with Dnmt family members (Dnmt1 NP_001186360, Dnmt3a NP_031898, Dnmt3b NP_001003961 and Dnmt3l NP_062321) or HMTs (Histone Methyl Transferase) on histone H3K9 (Eset NP_001157113.1, G9a NP_665829.1, Glp NP_001012536.2, Riz1 NP_001074854.3, Suv39h1 NP_035644.1, Suv39h2 NP_073561.2), but did not identify any similarities with ECAT15s. Recently, it has been indicated that Tet family members (Tet1

NP_081660.1, Tet2 NP_001035490.2 and Tet3 NP_898961.2) might have DNA demethylation ability through methyl cytosine oxidization **(9)**. Thus, the amino acid sequence of SAP domains and C-terminal regions of ECAT15-1 and ECAT15-2 were compared with the oxigenase domain of Tet family, but again, there are no significant similarities. There have been no reports that SAP motif-containing proteins have DNA or histone demethylation ability. Thus ECAT15s per se might not regulate epigenetic statuses.

Alternatively ECAT15s may bind and regulate other proteins involved in DNA methylation and histone modification. BioGRID (http://thebiogrid.org, version 3.1 on Dec. 12, 2010) predicts that human ECAT15-2 protein interacts with SETD5 (Set domain containing 5). SET domain is known as a methyltransferase domain, mainly for histone. Further studies are required to determine whether ECAT15s associate with SETD5 or other epigenetic modifying proteins and regulate their functions.

We detected aberrant epigenetic status in ECAT15-2 mutant ESCs, but not in mutant lungs. The promoter regions of *Gata4*, *Nkx2-5*, and *Syce1* seemed active judging from DNA hypo-methylation and H3K9me2 hypo-methylation in ECAT15-2 mutant lungs. Considering the suppressed expression of these genes in ECAT15-2 mutant lungs, the low DNA histone and DNA methylation statuses of these genes are paradoxical. One possibility is that these genes are expressed in a small cell population within lungs, and

thus analyses using whole lung lysates failed to detect epigenetic abnormalities in minor cell types. Another possibility is that other types of epigenetic marks, such as other histone tail modifications, are involved. Alternatively, ECAT15 proteins might regulate the expression of these genes through regulatory elements such as enhancers and suppressors, which we did not analyze in the current study. Further experiments are required to determine the precise mechanisms how ECAT15 proteins affect gene expression in organs in which they are no longer expressed.

Another unanswered question is functional interactions of the two ECAT15 proteins. They have 32% identities in amino acid sequences and have the common SAP domain. They physically interact with each other. Their expression patters are also similar. These suggest that the two proteins may have overlapping and compensatory functions. In contrary to this prediction, either ECAT15-1 or ECAT15-2 single deletion resulted in respiratory failure, suggesting that each protein has non-compensating roles in normal lung functions. We also found that deletion of both genes did not worsen the lung phenotypes. Rather, the double mutant resulted in a similar phenotype to that in ECAT15-1 single mutant lungs, which is milder than that observed in ECAT15-2 single mutant lungs. One model to explain this result is that ECAT15-1 has both supportive and detrimental effects in lung functions. The model predicts that the supportive effect also depends on ECAT15-2 protein whereas the detrimental effect is antagonized by

328 ECAT15-2. In this model, ECAT15-2 mutant lungs would suffer not only from the loss of
329 supportive effect of ECAT15s, but also from unmask of the detrimental effect of
330 ECAT15-1, which would become apparent due to loss of protection by ECAT15-2. In
331 contrast, double mutant lungs would suffer only from the loss of supportive effect of
332 ECAT15s.

333 This putative detrimental effect of ECAT15-1, which is antagonized by
334 ECAT15-2, may also exist in ESCs. We found that the deletion of ECAT15-2 showed
335 abnormality in proliferation **(Supplementary figure 6C)**. In addition, over-expression of
336 ECAT15-1 results in cell death during differentiation **(15)**. In contrast, ECAT15-1 single
337 and ECAT15-1/-2 double mutant ESCs are apparently normal **(11)**. Thus, like in lung,
338 the stoichiometric balance of the two ECAT15 proteins might be important for proper
339 functions of ESCs. When ECAT15-2 is suppressed, or when ECAT15-1 is overexpressed,
340 this balance might be destroyed and detrimental effects of ECAT15-1 become apparent.

341 Except for the slower proliferation of ECAT15-2 mutant ESCs, we found that
342 ECAT15 proteins are dispensable in mouse ESCs and pre-implantation embryos despite
343 its specific expression: even ECAT15-1/15-2 mutant peri-implantation embryos are
344 apparently normal. This result is consistent with the previous report that ECAT15-1
345 single mutant ESCs and ECAT15-1/15/2 double mutant ESCs were normal **(11)**.
346 However, ECAT15 proteins do regulate gene expression in ESCs, since DNA microarray

analyses detected many genes, including those involved in germ cell development, which are down-regulated in either ECAT15-1mutant ESCs **(11)** or ECAT15-2 mutant ESCs **(Supplementary figure 6E)**. Mutant ESCs may have developed compensate mechanisms, by which they can maintain pluripotency regardless of the altered gene expression. In contrast to our results, shRNA-mediated knockdown of ECAT15-1 or ECAT15-2 induced differentiation of mouse ESCs **(4, 7, 15)**. Reasons for this discrepancy remain to be determined.

The suppression of germ cell associated genes in mutant ESCs and significant expression in genital ridges in embryos, as well as in adult testes and ovaries, suggests that ECAT15s have important roles in germ cell development and gametogenesis. However, with the systemic gene targeting systems we used in this study, we obtained only a few ECAT15 homozygous mutant adult mice and were unable to perform detailed analyses of gametogenesis. Germ cell-specific gene disruption of ECAT15s would answer this important question.

We found that the number of the 15-2KO embryos decreased even before birth, during E16.5~E18.5 **(Table 1A)**. This suggests that the 15-2KO embryo had defects in organs that are indispensable for this developmental stage, in addition to lung. In mutant lungs, we detected suppression of genes such as Nkx2.5 and GATA4, which are important for functional heart development **(22).** Thus we postulated that the decrease

in the number of homozygous mutant embryos during E16.5~E18.5 may be attributable to abnormal heart development. However, we found that the heart of the ECAT15-2 mutant E15.5 embryos beaten normally and showed normal expression levels of Nkx2-5 and Gata4 (data not shown). It is still possible that ECAT15-2 mutant hearts have abnormalities such as malformation of valves. However, it is more likely that other organs are affected in mutant embryos. Importantly, these results also demonstrated that several genes such as Nkx2-5 and Gata4 were regulated by ECAT15-2 in lung, but not in heart.

In conclusion, our results demonstrated that the nuclear protein ECAT15-2 is essential for normal development of lung, in which the gene is not expressed during organogenesis. We propose that this represents a novel mechanism of gene regulation through epigenetic memories from earlier developmental stages when ECAT15-2 is expressed. Many important questions remained to be solved: What is the precise nature of epigenetic marks? Why is the lung specifically affected? What is the relationship between ECAT15-1 and ECAT15-2? The ECAT15 double conditional targeting system developed in this study should be useful to answer these important questions.

<Figure legends>

Figure 1, Generation of ECAT15-1/15-2 single or double mutant mice using ECAT15 double conditional targeting system

(A) Schematic illustration of ECAT15 double conditional targeting. A ~70 kbp fragment digested from BAC targeting vector with Sal1 was introduced into RF8 ESCs.

(B) Screening of homologous recombineered ESCs and detection of non-homologous insertion site by Southern blotting. All genomic DNA which were digested by Ssp1 were loaded in one gel, and the membrane was separated after blotting. The left membrane was detected using a Hyg probe (Green box in Panel A) and the right membrane was detected by the ECAT15_3' probe (Orange box in Panel A). Upper band indicates the targeted allele (CT allele) and the lower band indicates the wild-type allele (WT allele).

(C) Confirmation of homologous recombination using Taqman probe based quantitative genomic PCR. Each Taqman probe for wild-type *ECAT15-1* or *ECAT15-2* loci was designed as described in panel A (*ECAT15-1*; blue box, *ECAT15-2*; red box). CT clones indicate the correctly recombineered and WT clones were not correctly recombineered clones examined by Southern blotting. Error bar indicates the SD of three experiments.

(D) Strategy of ECAT15-1 and/or ECAT15-2 deletion. 15-1$^{+/CT}$, 15-2$^{+/CT}$ mice were mated with EIIA-Cre or Rosa26-FLPe transgenic mice step by step as shown.

Figure 2, Respiratory disorder in ECAT15-1/15-2 mutant embryos

(A) Representative images of HE staining of lung sections at E18.5.

(B) Expression levels of Scgb1a1 and SP-C in the E18.5 lung were examined by qRT-PCR. Blue and red bars in the graph indicate the median and mean.

(C) Expression levels of Scgb1a1 and SP-C in the E18.5 lung were examined by immunohistochemistry with anti- Scgb1a1 and anti- SP-C antibody. Arrows indicate alveoli that have SP-C positive cells and disrupted architecture.
All scale bars = 100 μm

Figure 3, ECAT15 expression during lung organogenesis.

(A) Relative expression level of ECAT15-1 and ECAT15-2 in the undifferentiated ESCs, developing lungs and gonads were examined by qRT-PCR. RNA from developing lungs and gonads were mixtures of several individuals. The numbers under the graph indicates the embryonic day. Te; testis, Ov; Ovary, GR; genital ridge (did not distinguish testis and ovary). Error bar indicates the SD of three experiments.

(B) Serial axial-proximal sections of the whole embryo at E14.5 were stained by *in situ*

418 hybridization using antisense ECAT15-1 probe and sense ECAT15-1 probe.

419 (C) The lung and testis of offspring at E14.5 between the 15-2-EGFP transgenic mice
420 and C57 BL/6J. Genotypes were confirmed by genomic PCR.

421 (D) The EGFP positive cells from the trypsinized 15-2-EGFP transgenic lungs and testis
422 were examined by flow cytometory. Total 50,000 cells of testis and 500,000 cells of
423 lung were examined. Rhodamine filter was used for detection of auto-fluorescence.
424 All scale bars = 100 μm

425 **Figure 4, Global gene expression in the 15-2KO lung.**

426 (A) Transcriptome analysis by microarray using the total lung RNA of wild-type and the
427 15-2KO sibs at E18.5. Heat map shows the 106 probes which were differentially
428 expressed over two-fold between the wild-type and the 15-2KO lung. Color range
429 indicates log2 scale.

430 (B) Relative expression levels of Gata4, Nkx2-5, Pitx1 and Pitx2 in the lungs at E18.5
431 were examined by qRT-PCR. Gata6 was analyzed as an unchanged control that was
432 not differentially expressed in the microarray analysis. Red and blue dots in graph
433 indicate the median and mean.

434 **Figure 5, Aberrant epigenetic status in the 15-2KO ESCs.**

(A) Methylation status of five candidate gene promoters in wild-type and the 15-2KO ESCs. The numbers under panels indicated the percentage of methylated CpG dinucleotides.

(B) ChIP analysis using anti-H3K9me2 antibody. Precipitated DNA of the wild-type (WT) and the 15-2KO (KO) ESCs was examined by qPCR.

(C) ChIP analysis using anti-ECAT15-2 antibody. Precipitated DNA of the wild-type (WT) and the 15-2KO (KO) ESCs was examined by qPCR.
Error bar indicate the SD of three experiments.

Figure 6, Epigenetic analysis of the 15-2KO lung.

(A) DNA methylation status of five candidate gene promoters in wild-type and the 15-2KO lungs. Numbers under panels indicate the percentage of methylated CpG dinucleotides.

(B) ChIP analysis using anti-H3K9me2 antibody. Precipitated DNA from wild-type and the 15-2KO lungs were examined by quantitative PCR. Error bar indicates the SD of three experiments.

Figure 7, Molecular moieties of ECAT15-1 and ECAT15-2 in ESCs.

(A) Sub-localization of ECAT15-1 and ECAT15-2 in ESCs were examined by

immunocytochemistry using anti-ECAT15-1 or anti-ECAT15-2 antibody with anti-HP1α antibody. Nuclear was counterstained with Hoechist33342. White bar indicates 5 μm.

(B) Molecular interaction between ECAT15-1 and ECAT15-2 were examined by immunoprecipitation assay using anti-ECAT15-2 antibody with a nuclear protein lysate of wild-type and the 15-2KO ESCs. ECAT15-1 and ECAT15-2 were detected by immunoblotting with anti-ECAT15-1 and anti-ECAT15-2 antibody. Arrow head indicates ECAT15-1 protein (left panel) and ECAT15-2 protein (right panel).

Table 1, Genotyping analysis of offspring from an intercross of heterozygous mutant mice.

(A) Genotyping analysis of offspring from 15-1$^{+/-}$, 15-2$^{+/FRT}$ intercross.

(B) Genotyping analysis of offspring from 15-1$^{+/Flox}$, 15-2$^{+/-}$ intercross.

(C) Genotyping analysis of offspring from 15-1$^{+/-}$, 15-2$^{+/-}$ intercross.

Abnormality indicated offspring whose genomic DNA could not be extracted.

Time of weaning; 1~5 weeks of age.

<Experimental procedures>

Construction of ECAT15 double conditional targeting BAC vector

A BAC DNA pool of a mouse BAC library (Research Genetics Co., Cat#.96021) was screened according to the manufacturer's instruction. The yielded BAC DNA contains 140 kbp around the *ECAT15-1* and *ECAT15-2* locus. A loxP-pgk-Neo^r-loxP fragment (loxP-Neo cassette, Gene Bridge) was inserted into the *ECAT15-1* locus and a FRT-pgk-Hyg^r-FRT fragment (FRT-Hyg cassette, Gene Bridge) was inserted into the *ECAT15-2* locus by Red/ET recombination technology (Gene Bridge) according to the manufacturer's instruction. The BAC DNA modification of each locus was performed through six steps. First, the loxP-Neo cassette was inserted into the 3' locus of *ECAT15-1* and then the pgk-Neo part was excised with 294-Cre E.coli (Gene Bridge). Finally, the loxP-Neo cassette was again inserted into the 1st intron of *ECAT15-1* locus. The same steps were employed to insert the FRT-Hyg cassette into the modified *ECAT15-2* locus with 294-FLPe E.coli (Gene Bridge).

Generation of the ECAT15 mutant mice and the 15-2KO ESCs.

The ECAT15 double conditional targeting BAC vector was digested with Sal1, and introduced into RF8 ESCs by electroporation. The primers for probe amplification of southern blotting and real-time PCR based on Taqman probe analysis are listed in **supplementary table 2**. The two clones correctly recombined were injected into C57 BL/6J blastocysts, thus yielding

chimeric mice that transmitted the targeting allele through the germ line from both clones. The detailed modification steps are indicated in **Figure 1D**. The 15-2KO ESCs were established from the 15-1$^{+/CT}$, 15-2$^{+/-}$ intercrossing as described previously **(23)**. The primers for genotype PCR are listed in **supplementary table 2.**

Gene expression analysis

RT-PCR and westernblotting were performed as described previously **(12)**. The primers for RT-PCR are listed in **supplementary table 2**. For calculation of expression level by RT-PCR, each value was normalized by Nat1 signal values as internal control. The antibodies used for immunoblotting were anti-ECAT15-1 antibody (TMD-PB-DP4, Cosmo Bio), rabbit anti-ECAT15-2 antiserum (generated against 158 amino acids of mouse ECAT15-2), anti-Oct3/4 (sc-5279, Santa Cruz), anti-Sox2 **(14)**, anti-Sall4 **(23)**, anti-β-actin (A5441, Sigma), anti-mouse IgG-HRP (#7076, Cell Signaling), and anti-rabbit IgG-HRP (#7074, Cell Signaling).

Histological analysis

Extirpated lung were fixed with 4% paraformaldehyde/PBS at 4˚C overnight. They were embedded in paraffin and cut into 3 μm sections with a microtome. Sections were deparaffinized and stained with hematoxylin and eosin solution. For immunohistochemistory, sections were stained with Vectastain universal Elite ABC kit (Vector lab. Cat#. PK-6200) according to the manufacturer's instructions. Anti Scgb1b1 antibody (Santa Cruz, sc-9772) and anti SP-C antibody (Millipore,

AB3786) was used at 1/100 and 1/2,000 dilution. Paraffin embedded blocks and sections of mouse tissues for *in situ* hybridization (ISH) were obtained from Genostaff Co., Ltd. The following procedures for ISH were performed according to the manufacturer's instruction (Genostaff Co., Ltd.). Probes for ECAT15-1 were generated with RF8 ESC cDNA and primers listed in **supplementary table 2.**

ESC culture and Immunocytochemistry analysis

ESCs were harvested on gelatin coated dishes as described previously **(18)**. Immunocytochemistry was performed as described previously **(21)**. The primary antibodies used for immunocytochemistry were anti-ECAT15-1 antibody or anti-ECAT15-2 antiserum and anti-HP1α antibody **(17)**. Secondary antibodies were Cy3-conjugated anti rabbit IgG antibody (Invitrogen) and Alexa488-conjugated anti mouse IgG antibody (Invitrogen). The nuclei were stained with Hoechst33342 (1/10,000, Invitrogen). Fluorescent signals were observed using confocal microscopy (LSM710, Carl Zeiss).

Generation of the 15-2-EGFP transgenic ESC and mice.

For the 15-2-EGFP vector construction, the EGFP-FRT-PGK-Hyg^r-FRT cassette was inserted into the start codon of ECAT15-2 loci of ECAT15 BAC DNA. The 15-2-EGFP reporter ESCs were generated by introduction of the BAC vector into RF8 ESCs. The 15-2-EGFP reporter mice were generated by introduction of the BAC vector into 1 cell embryo C57 BL/6J. Then the

15-2-EGFP-Hyg^r transgenic mice were mated with Rosa26-FLPe transgenic mice in order to delete Hygromycine resistant gene, and the 15-2-EGFP transgenic mice were obtained. The 15-2-EGFP transgenic mice were genotyped by detection of EGFP cassette.

Flow cytometory

Whole testis and lung of 15-2-EGFP reporter embryo at E14.5 were digested with 0.25% trypsin/1mM EDTA for 20min at 37℃, and the EGFP signals were analyzed by JSAN flow cytometory (Bay Bioscience) as described previously **(8)**. The rhodamine filter was used for detection of auto-fluorescence.

DNA microarray.

Total RNA from each samples were labeled with Cy3. Samples were hybridized with a Whole mouse genome microarray 4 x 44K (Agilent, Cat#. G4122F) as described previously **(20)**. Data were analyzed with GeneSpring GX ver.11. Quantile normalization was performed. The gene ontology analysis was performed by NEXTBIO (http://www.nextbio.com) using an entity list (106 entities, **Supplementary Table 1B**). All reported microarray data have been deposited in the public database Gene Expression Omnibus (http://www.ncbi.nlm.nih.gov/geo/) under accession number GSE31584.

Bisulfate sequencing

Extracted genomic DNA from wild-type ESCs and the15-2KO counterparts were analyzed

as described previously **(12)**. The primers for bisulfate sequencing analysis are listed in **Supplementary table 2.**

Immunoprecipitation

Protein lysate was extracted from mouse ESCs by CelLytic NuCLEAR Extraction Kit (Sigma, NXTRACT-1KT) according to the manufacturer's instruction with small modification. The nuclei were lysed with high salt extraction buffer (10 mM Hepes pH 7.9, 1.5 mM $MgCl_2$, 10 mM KCl, 500 mM NaCl, 0.5 mM DTT, supplemented with Complete protease inhibitor cocktail (Roche, Cat# 11 697 498 001)) by sonication with a Biorupter (CosmoBio). The lysates were dialyzed in dialysis buffer (20 mM Hepes pH 7.9, 150 mM NaCl, 100 mM KCl, 0.2 mM EDTA, and 0.5 mM DTT, supplemented with Complete protease inhibitor cocktail). Then the protein samples were incubated with magnetic beads (Invitrogen, Cat.#112.03D) conjugated anti-ECAT15-2 antibody at 4˚C overnight. The beads were washed six times with dialysis buffer then boiled in SDS sample buffer (50 mM Tris-HCl pH 6.8, 12.5% glycerol, 1% sodium dodecyl sulfate, 0.01% bromophenol blue, 5% β-mercaptoethanol) and separated by SDS-PAGE followed by immunoblotting as described above.

ChIP assay

We performed ChIP assay for ESCs as previously described **(12)**. Antibodies used in this experiment were anti-ECAT15-2 antiserum (also used for western blotting), anti-H3K4me3 antibody

(ab1012, Abcam), anti-H3K27me3 antibody (07-449, upstate), and anti-H3K9me2 antibody (ab1220, Abcam). We also performed ChIP assay with E18.5 whole lung tissue (P-2008-24, Epigentek) according to the manufacturer's instruction.

<Acknowledgments>

We thank T. Yamamoto, Y. Yamada, Y. Toda and the members of Yamanaka laboratory for valuable scientific discussions and administrative support. We thank T. Konishi, K. Iizuka, A. Okada, and M. Narita for technical assistance. This work was supported in part by Grants-in-Aid for Scientific Research from JSPS and MEXT. TN was a Research Fellow of the Japan Society for the Promotion of Science.

568 **<References>**

569 1. **Aravind, L., and E. V. Koonin.** 2000. SAP - a putative DNA-binding motif involved in
570 chromosomal organization. Trends in Biochemical Sciences **25:**112-114.
571 2. **Bannister, A. J., P. Zegerman, J. F. Partridge, E. A. Miska, J. O. Thomas, R. C. Allshire, and T.**
572 **Kouzarides.** 2001. Selective recognition of methylated lysine 9 on histone H3 by the HP1 chromo
573 domain. Nature **410:**120-124.
574 3. **Bortvin, A., K. Eggan, H. Skaletsky, H. Akutsu, D. L. Berry, R. Yanagimachi, D. C. Page, and R.**
575 **Jaenisch.** 2003. Incomplete reactivation of Oct4-related genes in mouse embryos cloned from
576 somatic nuclei. Development **130:**1673-1680.
577 4. **Du, J., T. Chen, X. Zou, B. Xiong, and G. Lu.** 2009. Dppa2 Knockdown-induced Differentiation and
578 Repressed Proliferation of Mouse Embryonic Stem Cells. J Biochem.
579 5. **Farley, F. W., P. Soriano, L. S. Steffen, and S. M. Dymecki.** 2000. Widespread recombinase
580 expression using FLPeR (flipper) mice. Genesis **28:**106-110.
581 6. **Glasser, S. W., M. S. Burhans, T. R. Korfhagen, C. L. Na, P. D. Sly, G. F. Ross, W. Ikegami, and J.**
582 **A. Whitsett.** 2001. Altered stability of pulmonary surfactant in SP-C-deficient mice. Proceedings
583 of the National Academy of Sciences of the United States of America **98:**6366-6371.
584 7. **Ivanova, N., R. Dobrin, R. Lu, I. Kotenko, J. Levorse, C. DeCoste, X. Schafer, Y. Lun, and I. R.**
585 **Lemischka.** 2006. Dissecting self-renewal in stem cells with RNA interference. Nature
586 **442:**533-538.
587 8. **Iwabuchi, K. A., T. Yamakawa, Y. Sato, T. Ichisaka, K. Takahashi, K. Okita, and S. Yamanaka.**
588 2011. ECAT11/L1td1 is enriched in ESCs and rapidly activated during iPSC generation, but it is
589 dispensable for the maintenance and induction of pluripotency. PLoS One **6:**e20461.
590 9. **Koh, K. P., A. Yabuuchi, S. Rao, Y. Huang, K. Cunniff, J. Nardone, A. Laiho, M. Tahiliani, C. A.**
591 **Sommer, G. Mostoslavsky, R. Lahesmaa, S. H. Orkin, S. J. Rodig, G. Q. Daley, and A. Rao.** 2011.
592 Tet1 and Tet2 regulate 5-hydroxymethylcytosine production and cell lineage specification in
593 mouse embryonic stem cells. Cell Stem Cell **8:**200-213.
594 10. **Leneuve, P., S. Colnot, G. Hamard, F. Francis, M. Niwa-Kawakita, M. Giovannini, and M.**
595 **Holzenberger.** 2003. Cre-mediated germline mosaicism: a new transgenic mouse for the selective
596 removal of residual markers from tri-lox conditional alleles. Nucleic Acids Research **31**.
597 11. **Madan, B., V. Madan, O. Weber, P. Tropel, C. Blum, E. Kieffer, S. Viville, and H. J. Fehling.** 2009.
598 The pluripotency-associated gene Dppa4 is dispensable for embryonic stem cell identity and germ
599 cell development but essential for embryogenesis. Mol Cell Biol **29:**3186-3203.
600 12. **Maekawa, M., K. Yamaguchi, T. Nakamura, R. Shibukawa, I. Kodanaka, T. Ichisaka, Y.**
601 **Kawamura, H. Mochizuki, N. Goshima, and S. Yamanaka.** 2011. Direct reprogramming of somatic
602 cells is promoted by maternal transcription factor Glis1. Nature **474:**225-229.
603 13. **Maldonado-Saldivia, J., J. van den Bergen, M. Krouskos, M. Gilchrist, C. Lee, R. Li, A. H. Sinclair,**
604 **M. A. Surani, and P. S. Western.** 2007. Dppa2 and Dppa4 are closely linked SAP motif genes

restricted to pluripotent cells and the germ line. Stem Cells **25:**19-28.

14. **Maruyama, M., T. Ichisaka, M. Nakagawa, and S. Yamanaka.** 2005. Differential roles for sox15 and sox2 in transcriptional control in mouse embryonic stem cells. J Biol Chem **280:**24371-24379.

15. **Masaki, H., T. Nishida, S. Kitajima, K. Asahina, and H. Teraoka.** 2007. Developmental pluripotency-associated 4 (DPPA4) localized in active chromatin inhibits mouse embryonic stem cell differentiation into a primitive ectoderm lineage. J Biol Chem **282:**33034-33042.

16. **Masaki, H., T. Nishida, R. Sakasai, and H. Teraoka.** 2010. DPPA4 modulates chromatin structure via association with DNA and core histone H3 in mouse embryonic stem cells. Genes to Cells **15:**327-337.

17. **Meshorer, E., D. Yellajoshula, E. George, P. J. Scambler, D. T. Brown, and T. Mistell.** 2006. Hyperdynamic plasticity in pluripotent embryonic of chromatin proteins stem cells. Developmental Cell **10:**105-116.

18. **Mitsui, K., Y. Tokuzawa, H. Itoh, K. Segawa, M. Murakami, K. Takahashi, M. Maruyama, M. Maeda, and S. Yamanaka.** 2003. The Homeoprotein Nanog Is Required for Maintenance of Pluripotency in Mouse Epiblast and ES Cells. Cell **113:**631-642.

19. **Nakamura, T., Y. Arai, H. Umehara, M. Masuhara, T. Kimura, H. Taniguchi, T. Sekimoto, M. Ikawa, Y. Yoneda, M. Okabe, S. Tanaka, K. Shiota, and T. Nakano.** 2007. PGC7/Stella protects against DNA demethylation in early embryogenesis. Nat Cell Biol **9:**64-71.

20. **Okita, K., T. Ichisaka, and S. Yamanaka.** 2007. Generation of germline-competent induced pluripotent stem cells. Nature **448:**313-U311.

21. **Takahashi, K., K. Tanabe, M. Ohnuki, M. Narita, T. Ichisaka, K. Tomoda, and S. Yamanaka.** 2007. Induction of pluripotent stem cells from adult human fibroblasts by defined factors. Cell **131:**861-872.

22. **Takeuchi, J. K., and B. G. Bruneau.** 2009. Directed transdifferentiation of mouse mesoderm to heart tissue by defined factors. Nature **459:**708-711.

23. **Tsubooka, N., T. Ichisaka, K. Okita, K. Takahashi, M. Nakagawa, and S. Yamanaka.** 2009. Roles of Sall4 in the generation of pluripotent stem cells from blastocysts and fibroblasts. Genes Cells **14:**683-694.

24. **Weaver, M., J. M. Yingling, N. R. Dunn, S. Bellusci, and B. L. Hogan.** 1999. Bmp signaling regulates proximal-distal differentiation of endoderm in mouse lung development. Development **126:**4005-4015.

25. **Wei Shi, S. B. a. D. W.** 2007. Lung Development and Adult Lung Diseases. Chest **132:**651-656.

26. **Woltjen, K., I. P. Michael, P. Mohseni, R. Desai, M. Mileikovsky, R. Hämäläinen, R. Cowling, W. Wang, P. Liu, M. Gertsenstein, K. Kaji, H. K. Sung, and A. Nagy.** 2009. piggyBac transposition reprograms fibroblasts to induced pluripotent stem cells. Nature **458:**766-770.

Figure 1

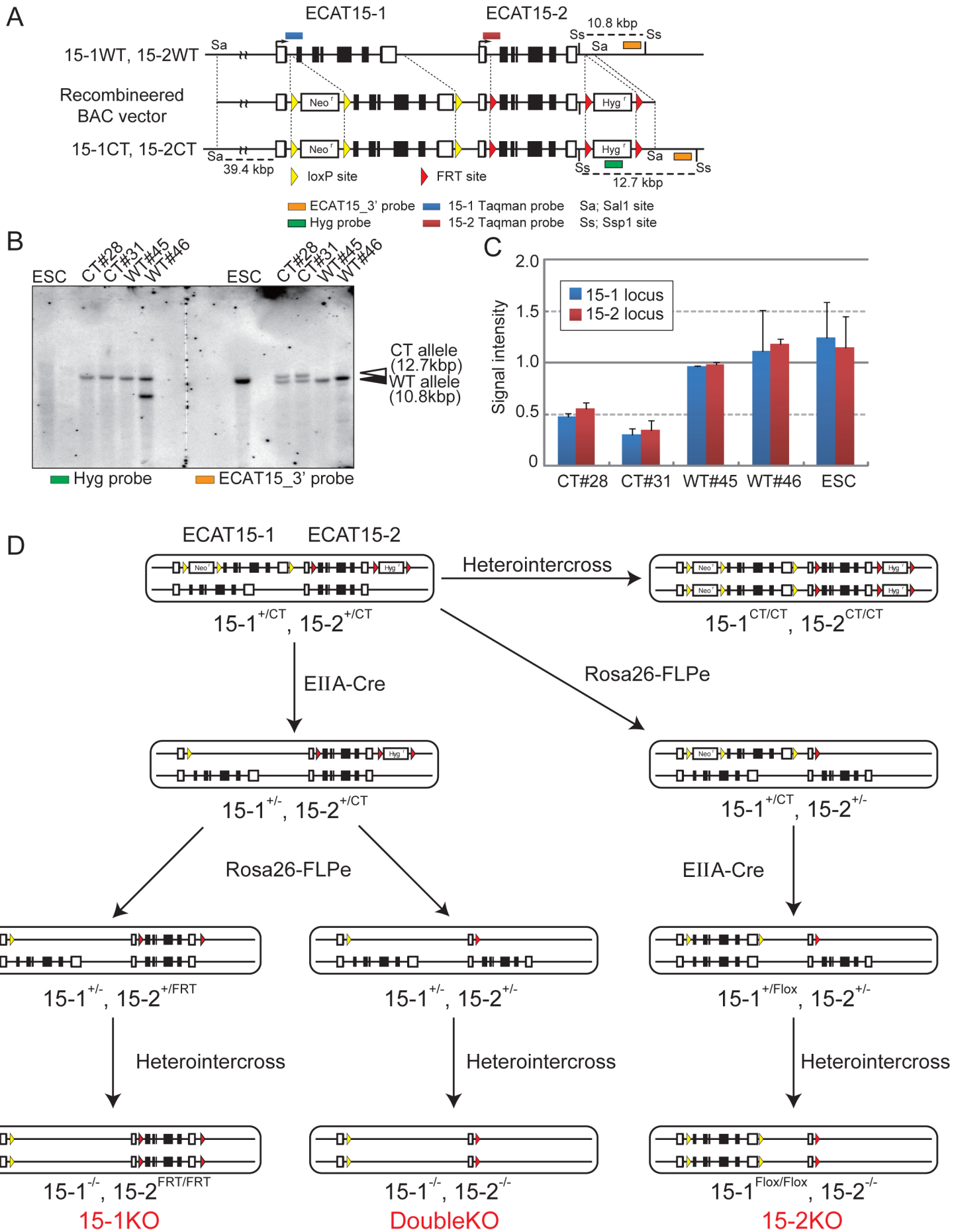

Figure 2

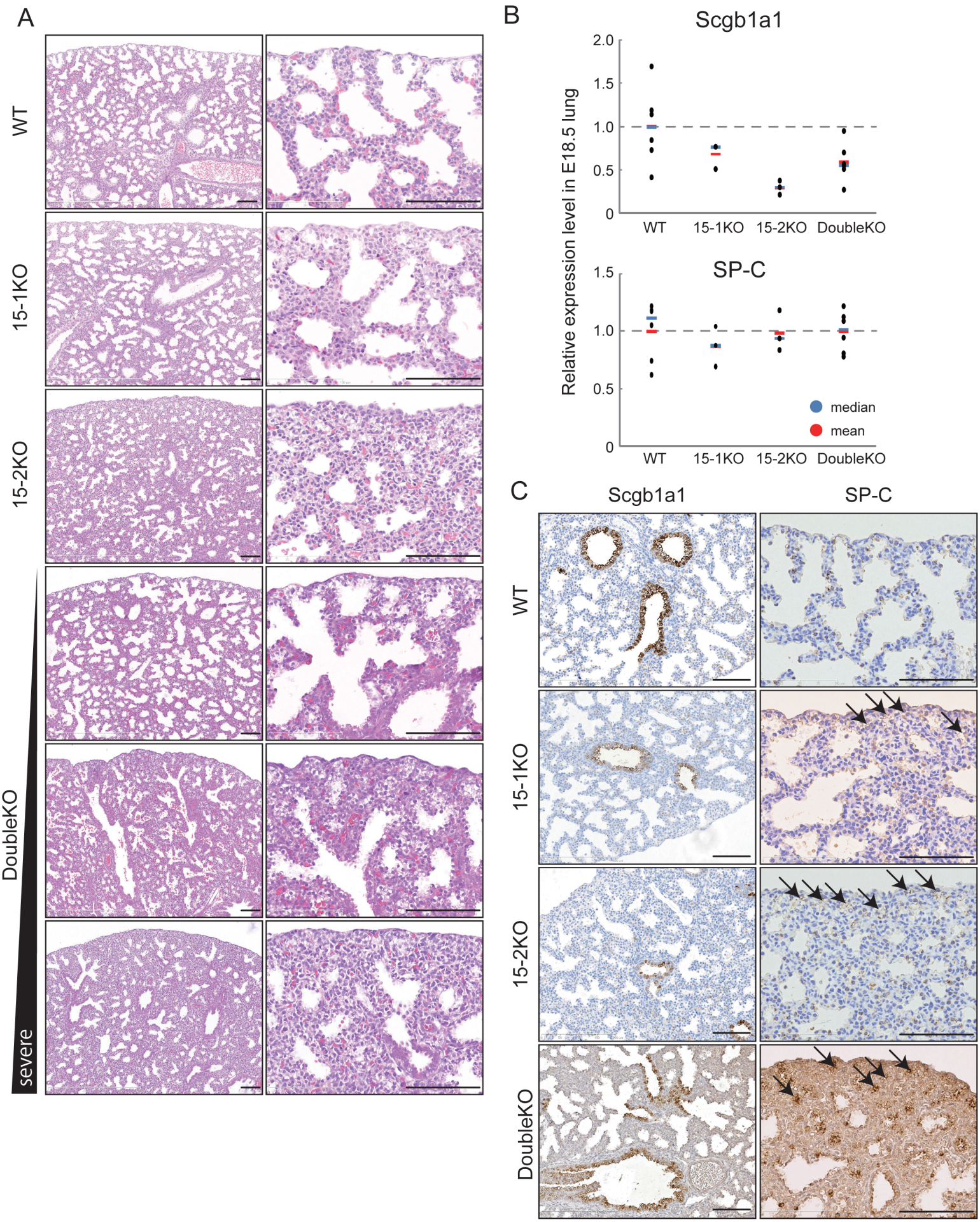

Figure 3

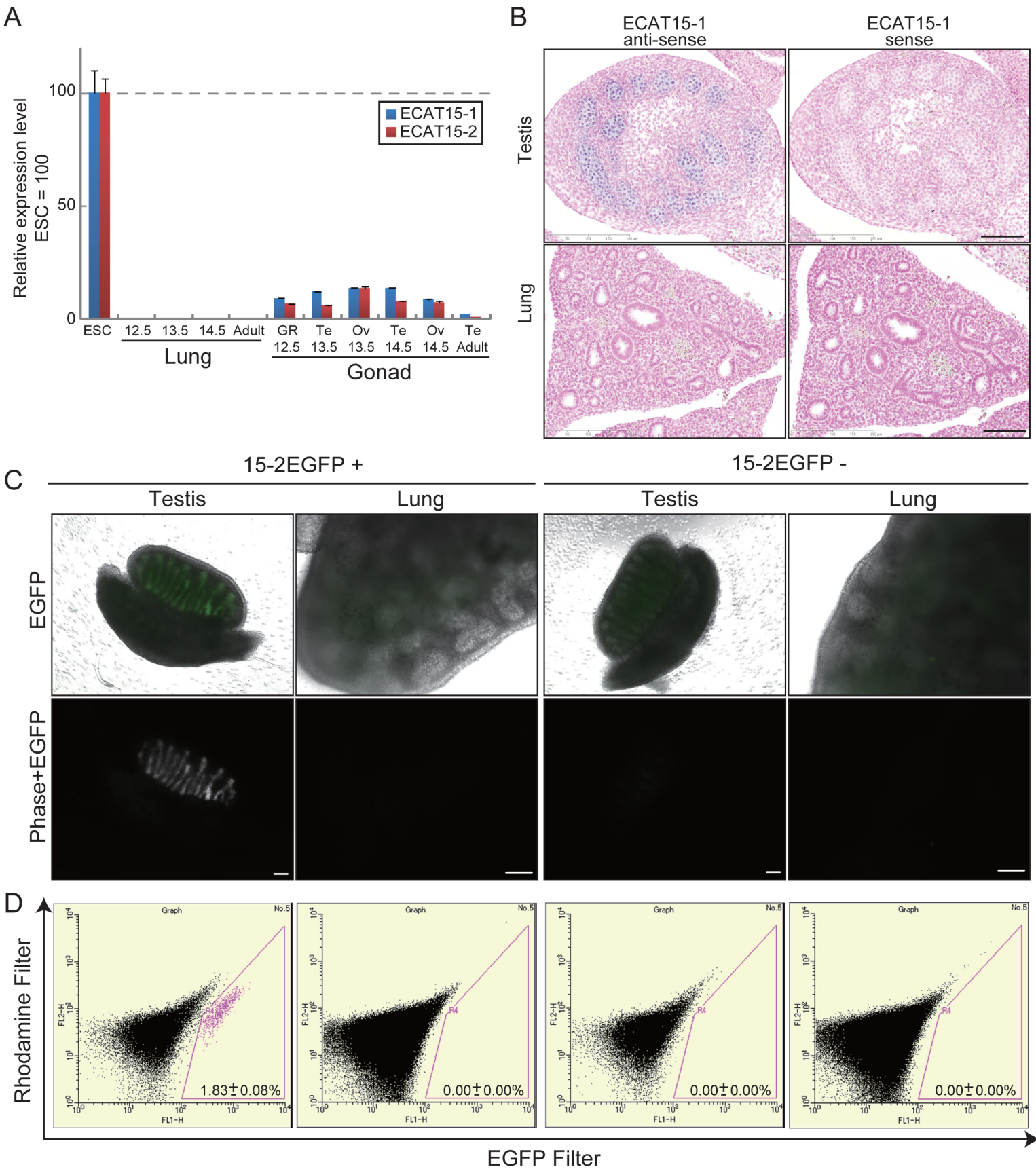

Figure 4

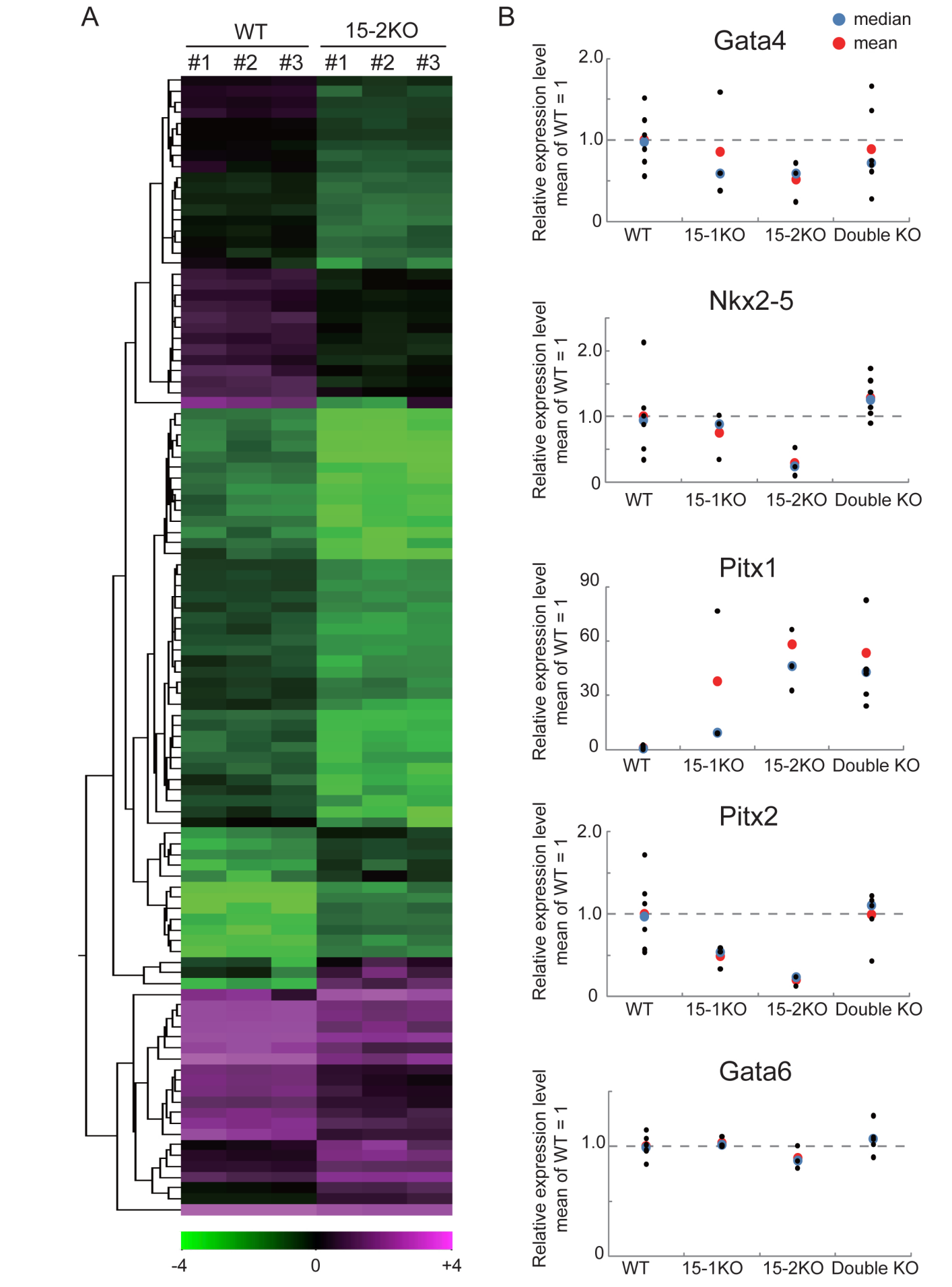

Figure 5

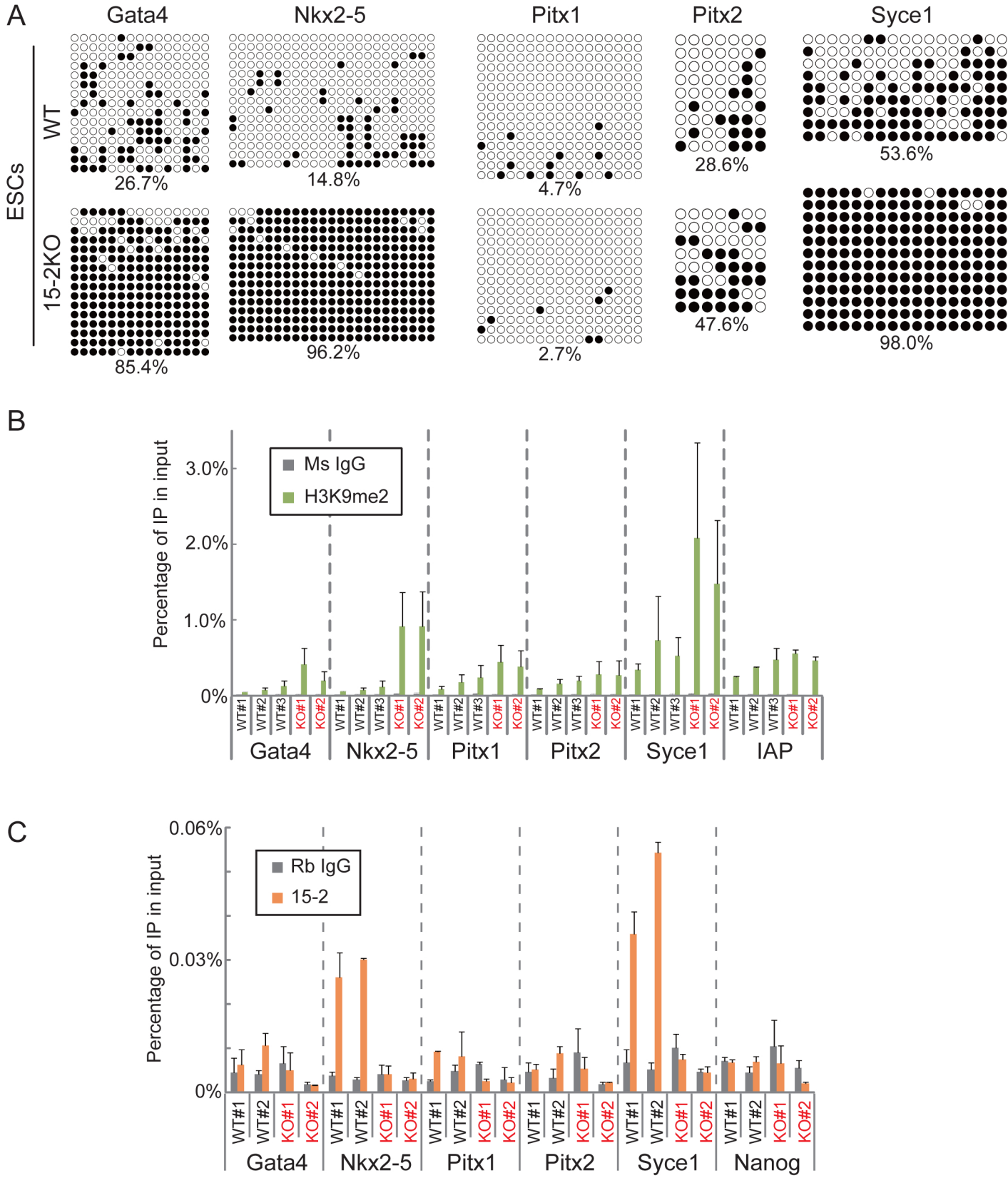

Figure 6

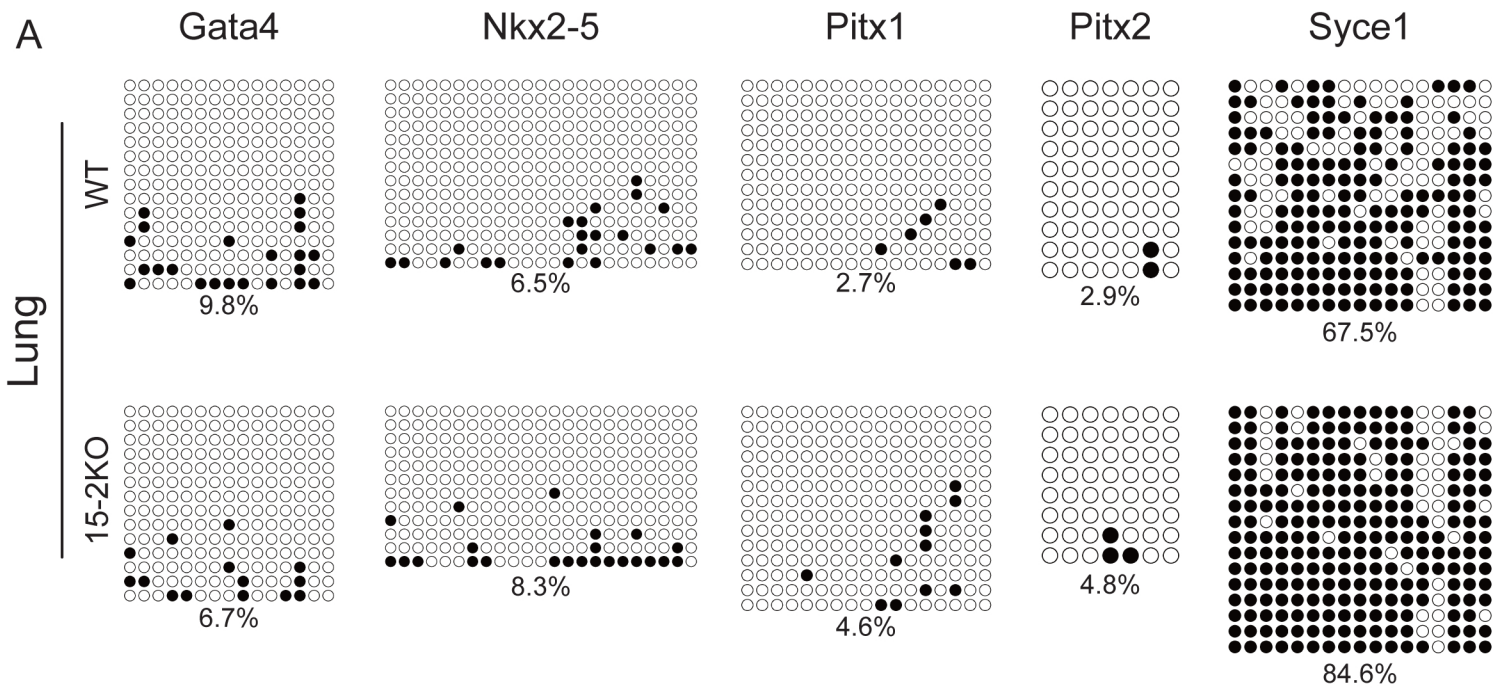

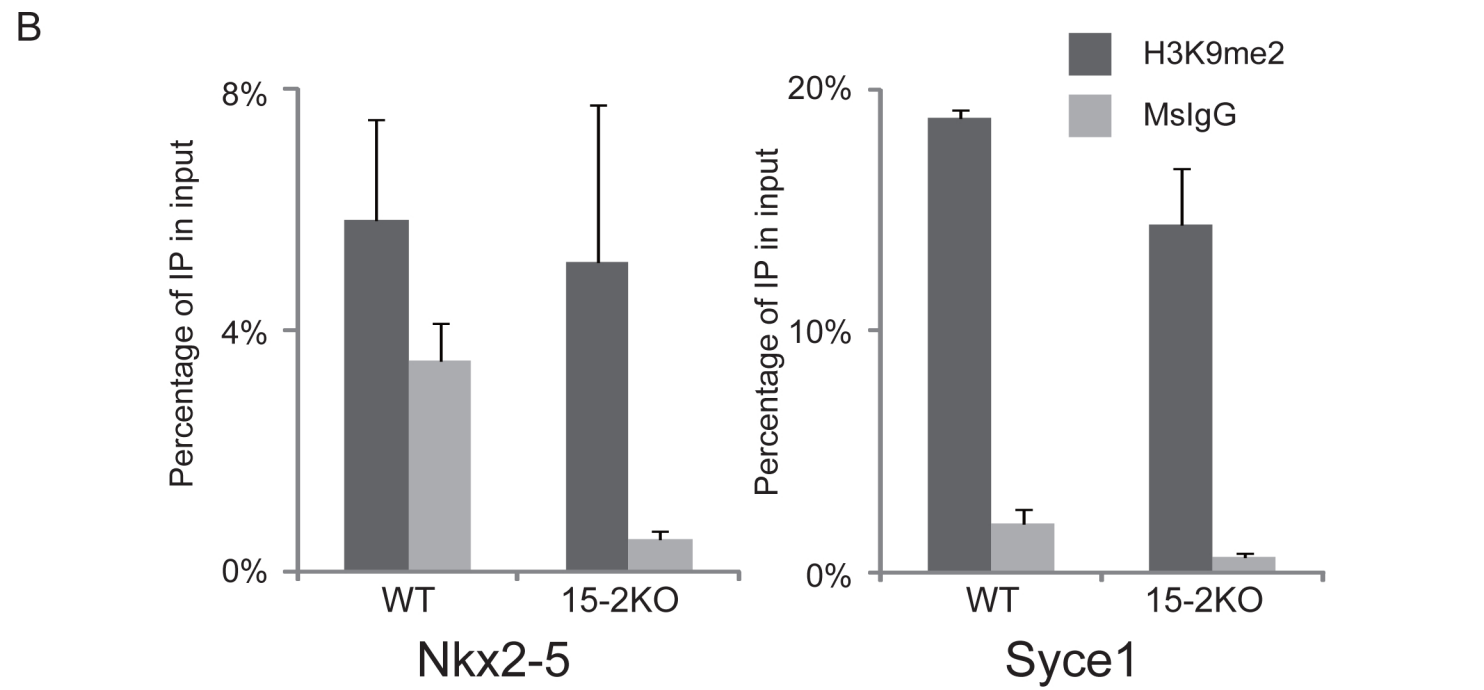

Figure 7

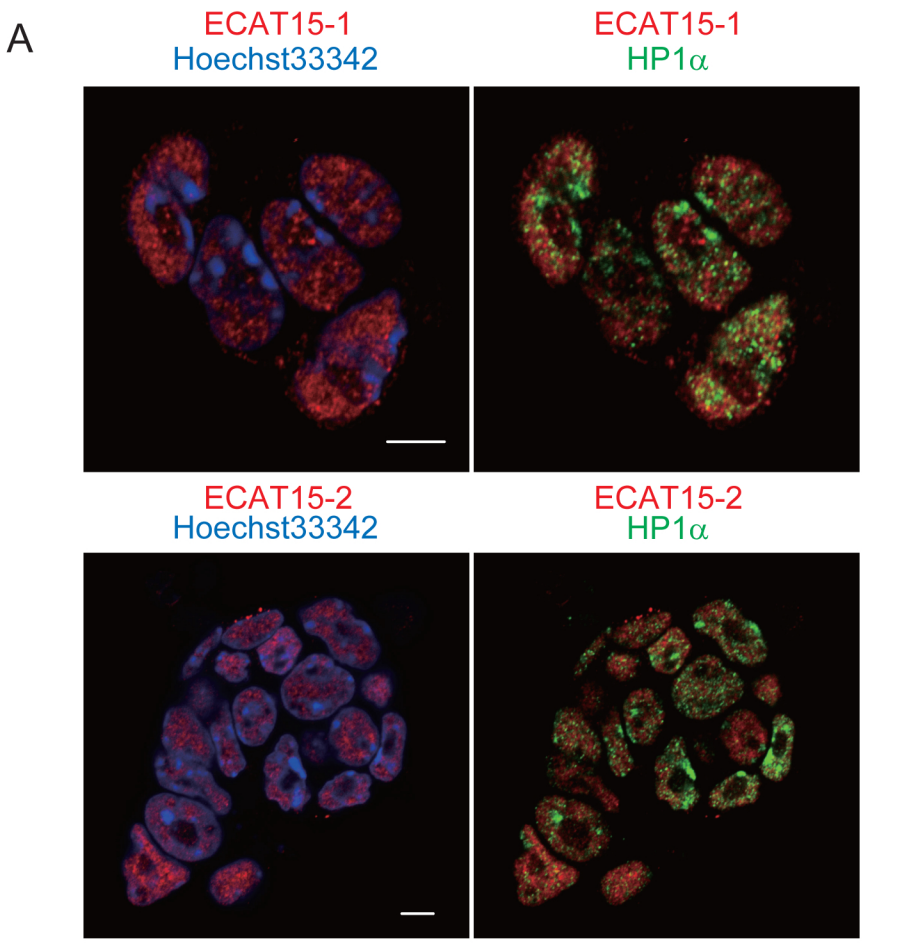

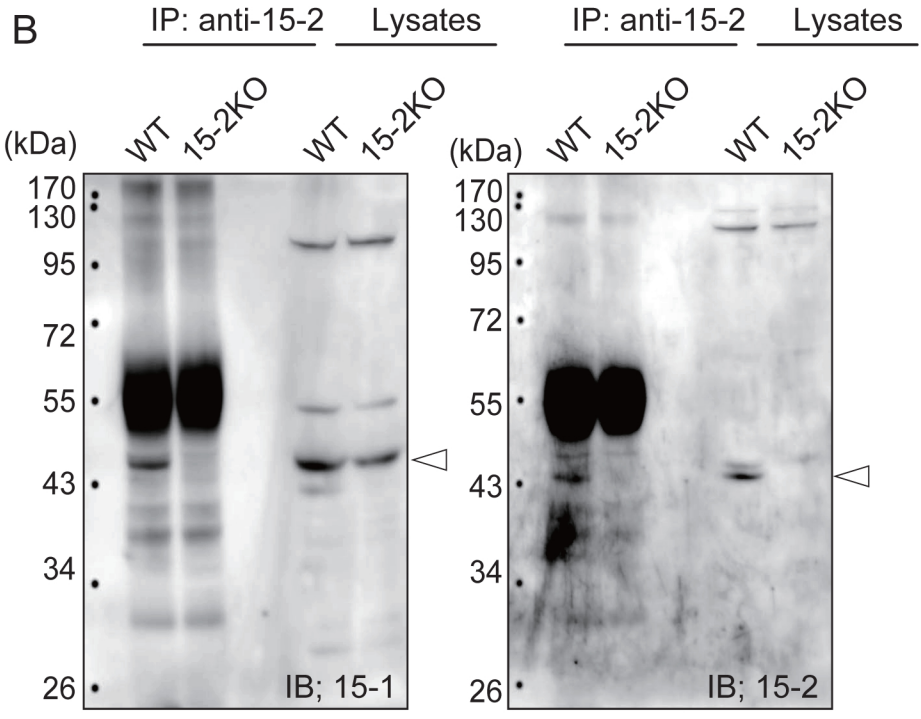

Table 1

A

15-1, 15-2		WT +/+, +/+	15-1Hetero +/-, +/FRT	15-1KO -/-, FRT/FRT	Abnormality
E18.5		16	27	11	6
P0	Alive	26	45	13	
	Dead	2	3	7	
1 week		27	66	0	
Time of weaning		128	281	14	

B

15-1, 15-2		WT +/+, +/+	15-2Hetero +/Flox, +/-	15-2KO Flox/Flox, -/-	Abnormality
E10.5		6	7	9	4
E12.5		10	12	4	7
E15.5		9	24	8	8
E16.5		4	15	6	7
E18.5		36	60	10	28
P0	Alive	10	29	2	
	Dead	1	2	3	
Time of weaning		153	290	0	

C

15-1, 15-2		WT +/+, +/+	DoubleHetero +/-, +/-	DoubleKO -/-, -/-	Abnormality
E16.5		9	30	10	5
E18.5		36	62	37	12
P0	Alive	20	33	7	
	Dead	0	1	2	
Time of weaning		152	286	13	

Nakamura et al.

Supplementary Figure 1

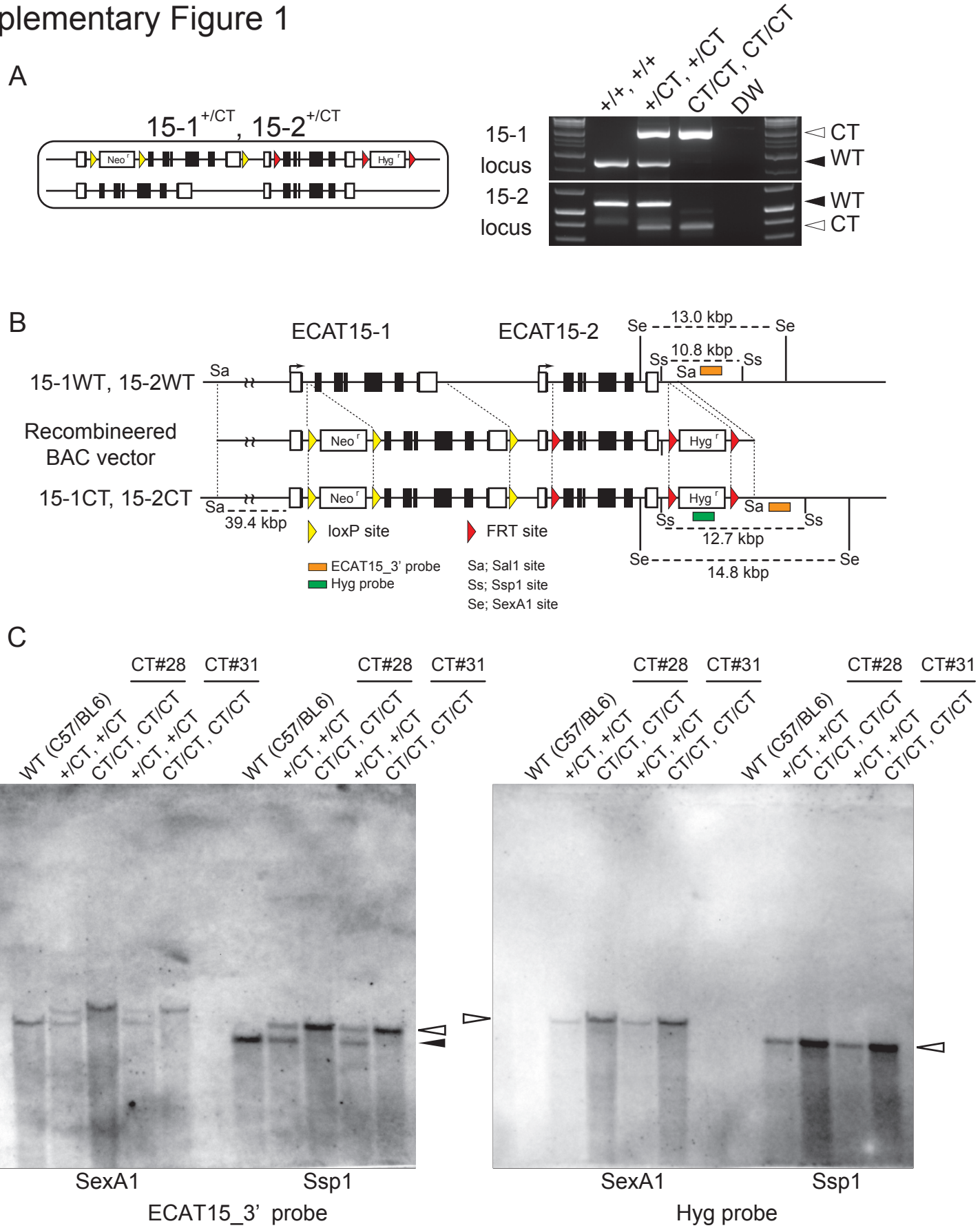

Supplementary Figure 1, Genotype of ECAT15 double conditional mutant mice.
(A) Schematic illustration of the 15-1$^{+/CT}$, 15-2$^{+/CT}$ and the genotype PCR of offspring from the heterointercross.
(B) Schematic illustration of ECAT15 double conditional targeting. The digested site by SexA1 and Ssp1 are indicated in panel as Se and Ss.
(C) Southern blot analysis using genomic DNAs from CT#28 and CT#31 derived mice. Those genomic DNAs were digested by SexA1 and Ssp1 restriction enzymes. Left membrane was hybridized with ECAT15_3' probe, right one was done with Hyg probe. White and black arrow heads indicate the bands of CT allele and WT allele.

Supplementary Figure 2

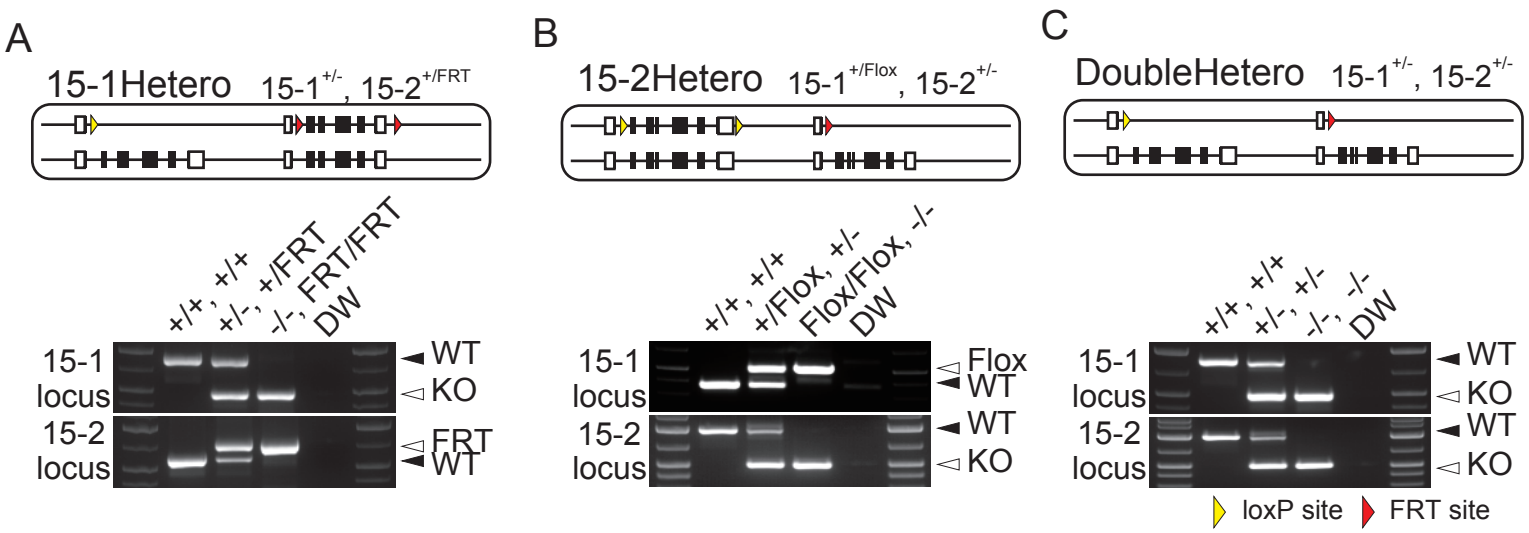

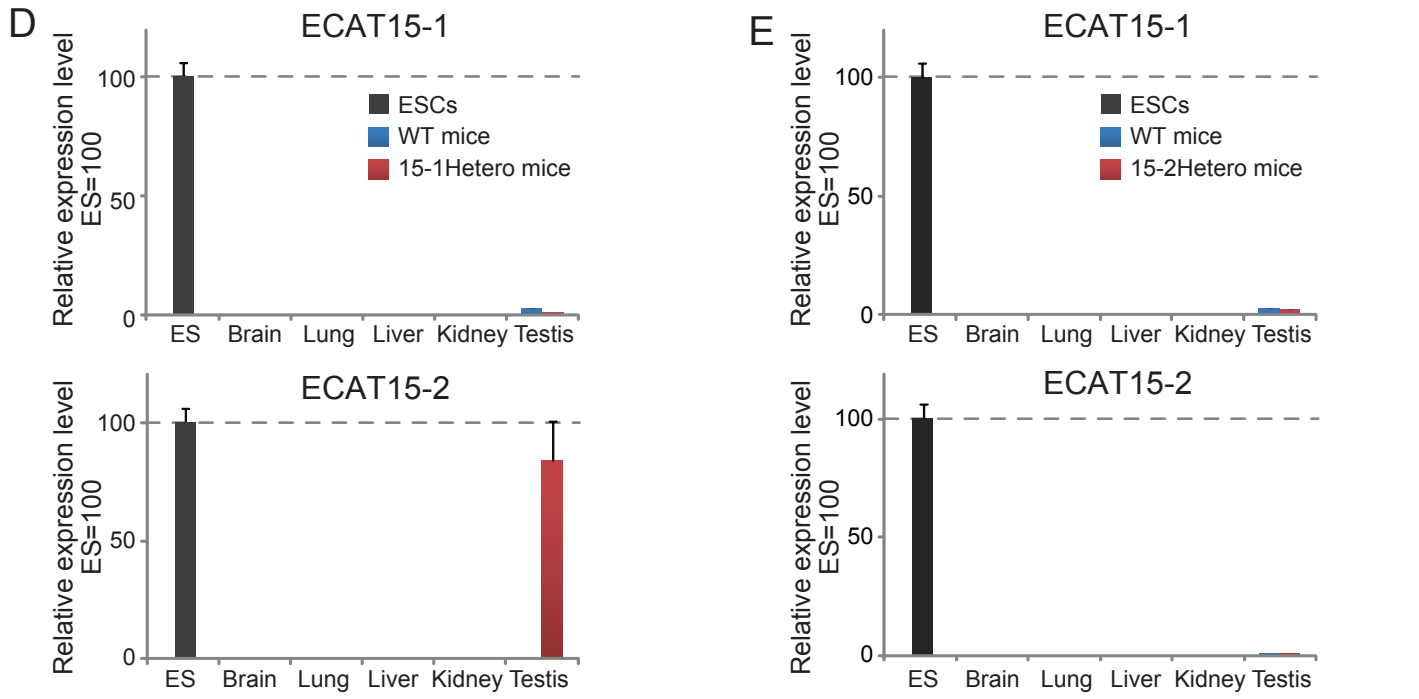

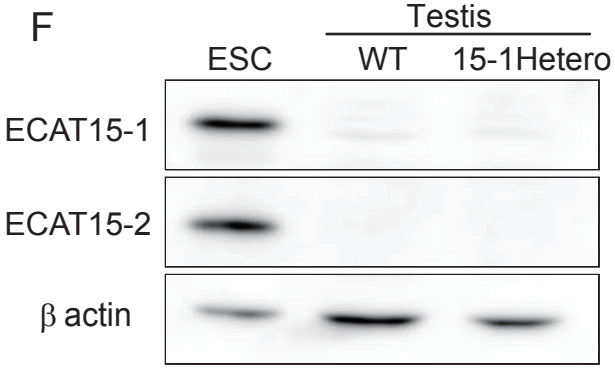

Supplementary Figure 2, Expression from 15-1Flox and 15-2FRT allele.

(A-C) Schematic illustration of the 15-1$^{+/-}$, 15-2$^{+/FRT}$ (A), the 15-1$^{+/Flox}$, 15-2$^{+/-}$ (B) and the 15-1$^{+/-}$, 15-2$^{+/-}$ (C), and the genotype PCR of offspring from each heterointercross.

(D) Relative mRNA expression levels of ECAT15-1 and ECAT15-2 in tissues of wild-type and the 15-1$^{+/-}$, 15-2$^{+/FRT}$ mice were examined by qRT-PCR.

(E) Relative mRNA expression levels of ECAT15-1 and ECAT15-2 in tissues of wild-type and the 15-1$^{+/Flox}$, 15-2$^{+/-}$ mice were examined by qRT-PCR. Error bar indicates the SD of three experiments.

(F) Protein expression of ECAT15-1 and ECAT15-2 in the undifferentiated ESCs and the testis lysate from wild-type and the 15-1$^{+/-}$, 15-2$^{+/FRT}$ mice were examined by immunoblot analysis.

Nakamura et al.

Supplementary Figure 3

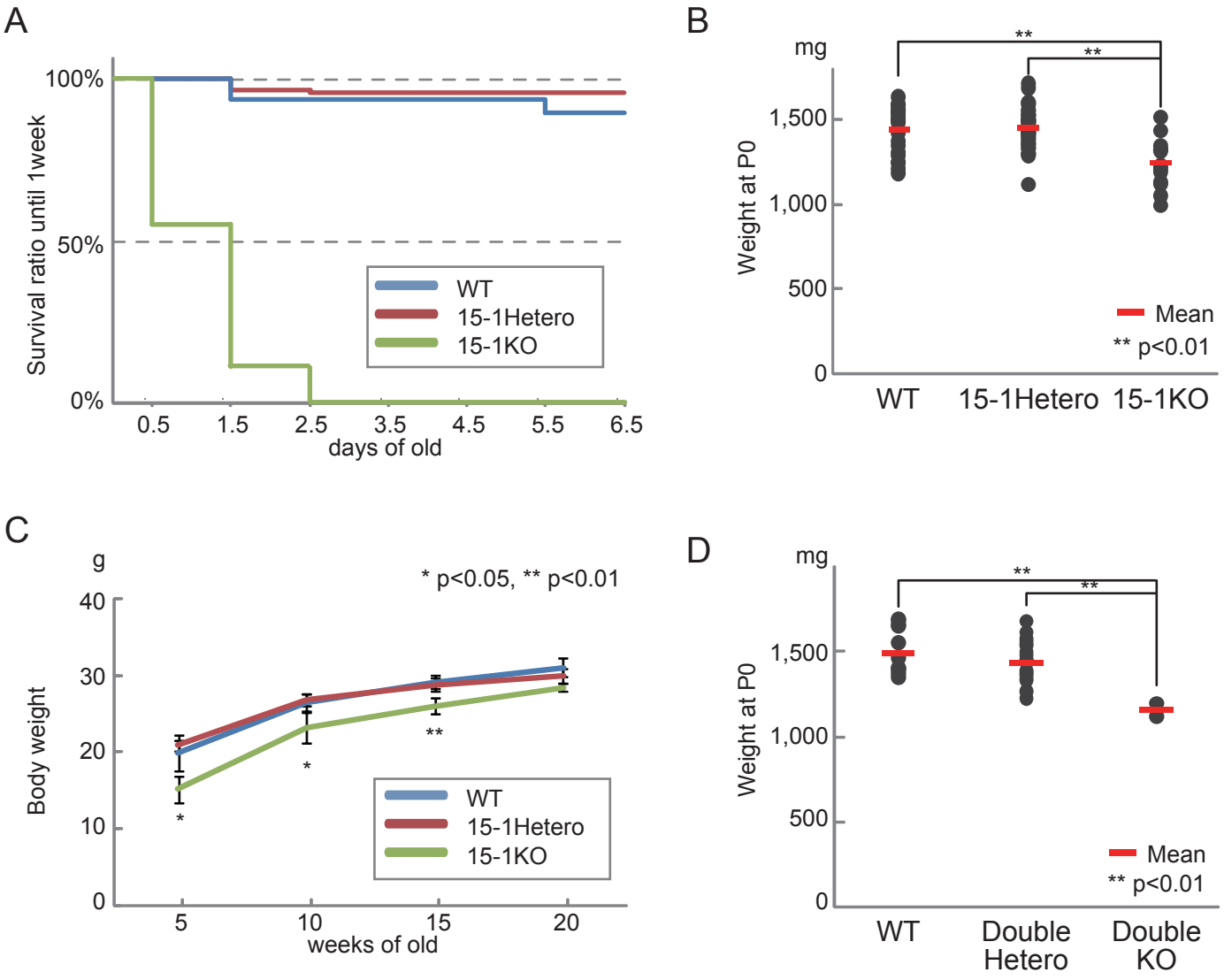

Supplementary Figure 3, Analysis of the 15-1KO and the DoubleKO neonates

(A) Survival ratio of offspring from the 15-1$^{+/-}$, 15-2$^{+/FRT}$ mice intercrossing was calculated by the Kaplan-Meier estimate. Note that the Numbers of pups on 9 o'clock in the birthday were set as 100%, thus the dead pups before 9 o'clock were not taken into account.

(B) Body weight of offspring at P0 from the 15-1$^{+/-}$, 15-2$^{+/FRT}$ mice intercrossing. The statistical analysis was performed with one-way ANOVA and the post-hoc test Bonferroni.

(C) Time course graph of the body weight of neonates from the 15-1$^{+/-}$, 15-2$^{+/FRT}$ mice intercrossing. The statistical analysis among three genotypes was performed with one-way ANOVA and the post-hoc test Bonferroni.

(D) Body weight of offspring from the 15-1$^{+/-}$, 15-2$^{+/-}$ mice intercrossing. The statistical analysis was performed with one-way ANOVA and the post-hoc test Bonferroni.

Nakamura et al
Supplementary Figure 4

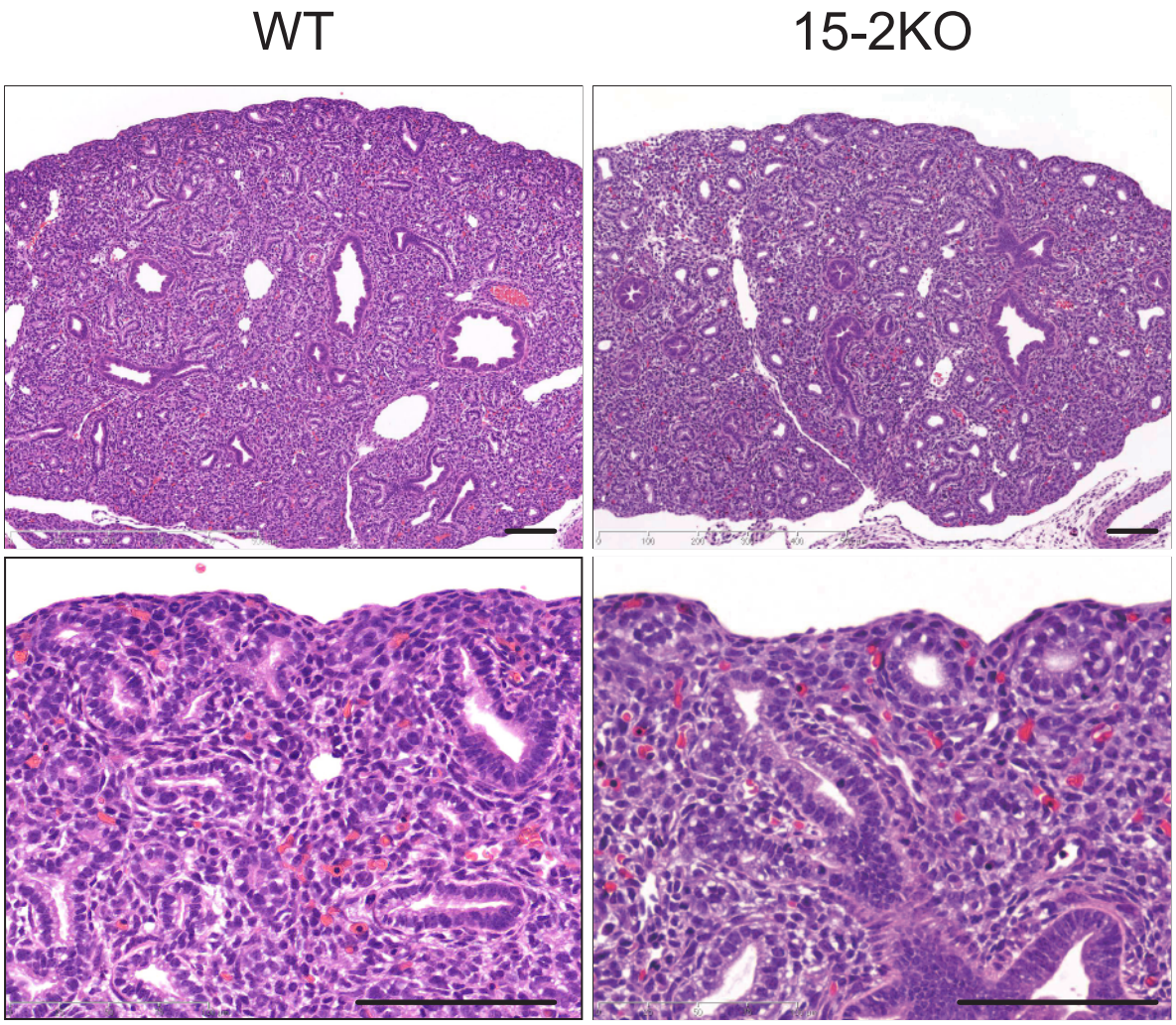

Supplemantary Figure 4, Histological analysis of the 15-2KO lung at E16.5
Representative image of HE staining. Offspring of 15-1$^{+/Flox}$, 15-2$^{+/-}$ intercrossing were disected and their lungs were sectioned and stained by Hematoxyline and eosin. Scale bar = 100μm.

Nakamura et al

Supplementary Figure 5

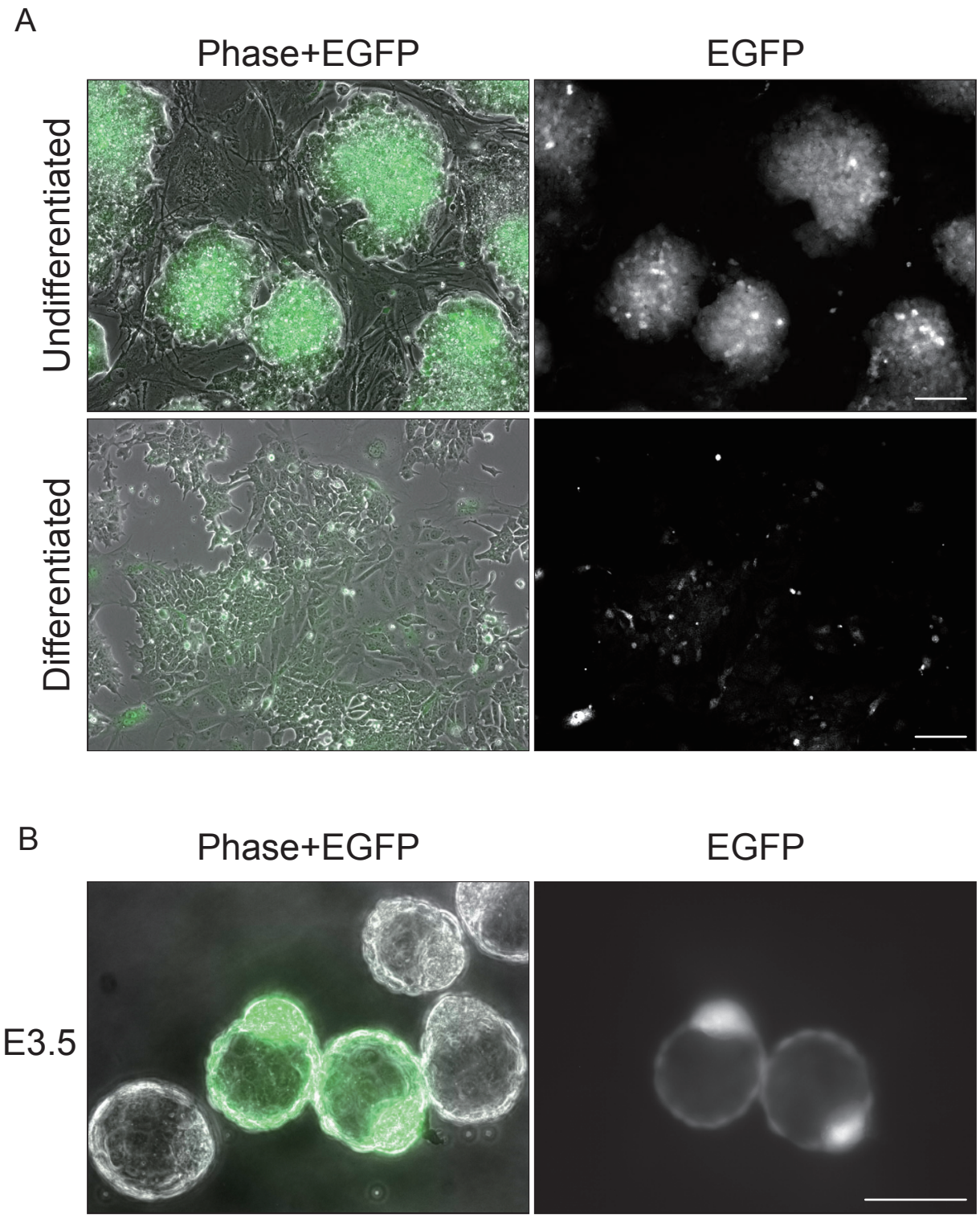

Supplemantary Figure 5, The 15-2-EGFP reporter in pluripotent cells.
(A) The 15-2-EGFP reporter ESCs. This ESC was maintained on SNL feeders (undifferentiated) or with neither LIF nor feeder cells (differentiated).
(B) Offspring at E3.5 between the male 15-2-EGFP transgenic mice and the female C57 BL/6J mice.
All scale bars = 100 μm

Nakamura et al

Supplementary Figure 6

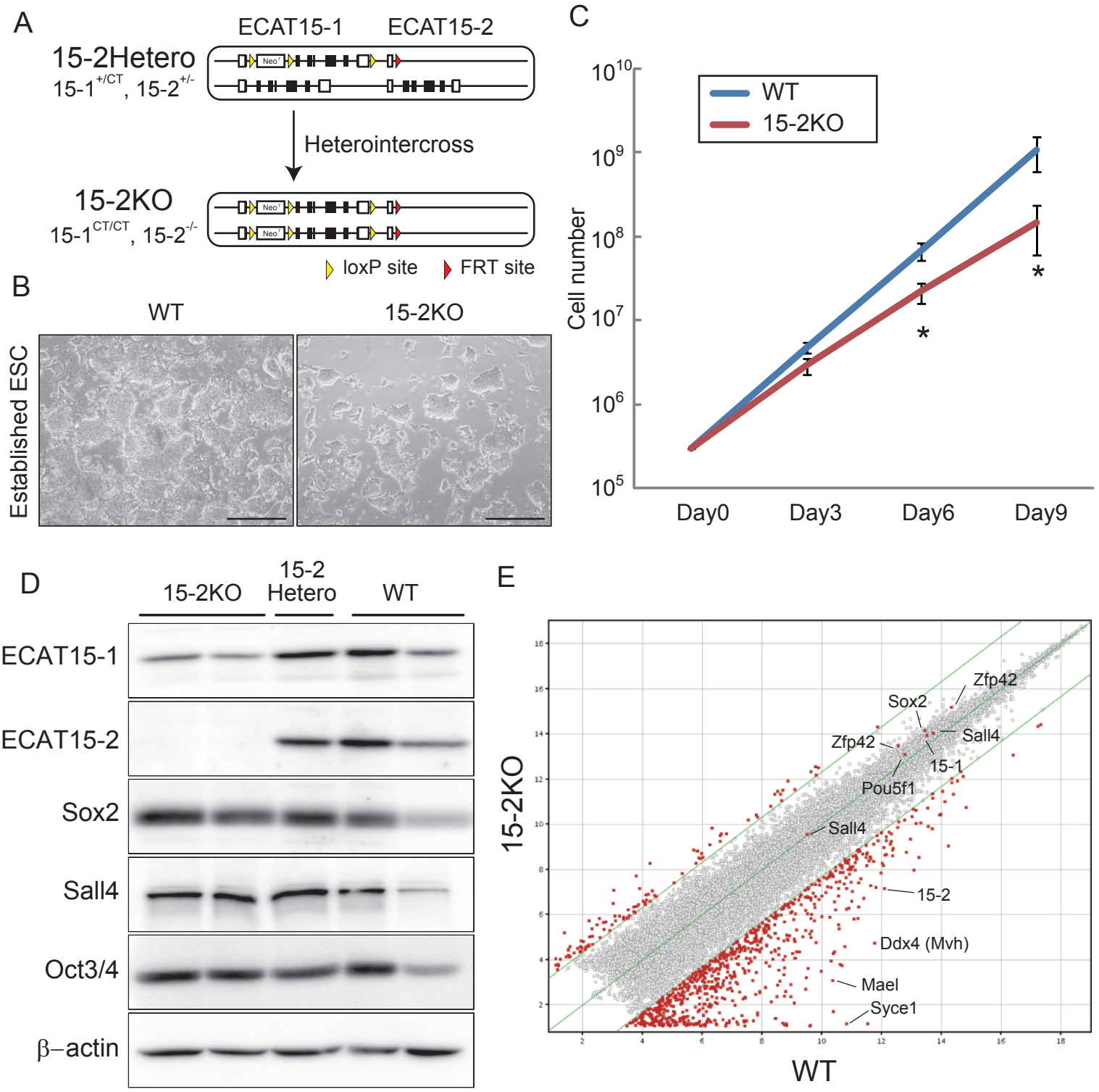

Supplementary Figure 6, Establishment of the 15-2KO ESCs.
(A) Schematic illustration of the 15-2KO (15-1$^{CT/CT}$, 15-2$^{-/-}$) ESC generation form 15-1$^{+/CT}$, 15-2$^{+/-}$ heterointercross.
(B) Morphology of the 15-2KO and wild-type sibling ESCs under undifferentiated conditions. Scale bar = 100μm
(C) Growth curve of the 15-2KO ESCs. The statistical analysis was performed with unpaired t-test. *, $p<0.05$
(D) Protein expression of ECAT15-1, ECAT15-2 and pluripotent markers.
(E) Two-dimensional scatter plot of log ratios of relative transcript levels by microarray analysis. Green bar indicated the borderline for 5 fold differences, and the Red dots indicated transcripts that were differentially expressed more than five fold between wild-type and the 15-2KO ESCs.

Supplementary Figure 7

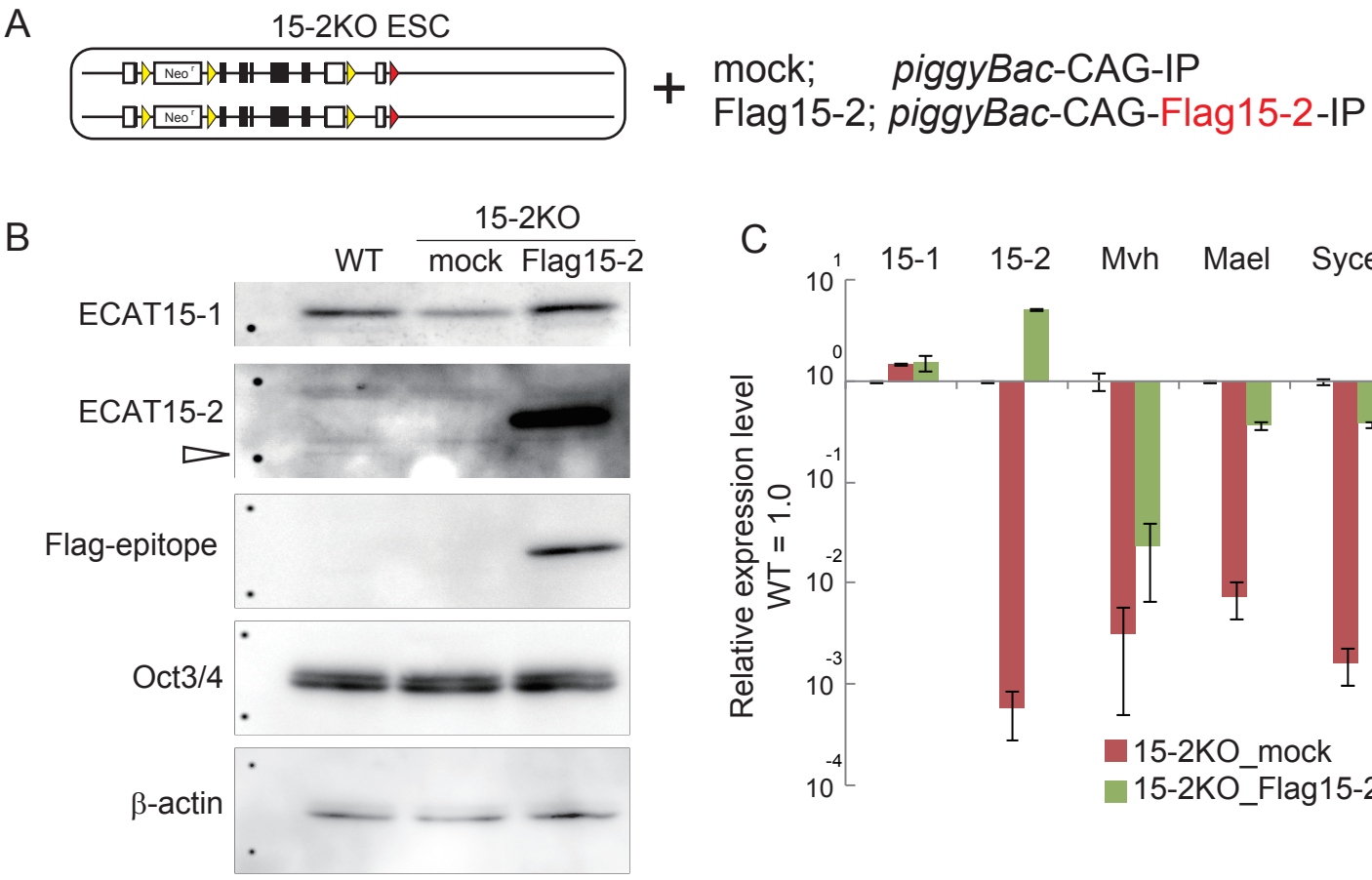

Supplementary Figure 7, Transgenic rescue experiment of ECAT15-2 expressing vector into the 15-2KO ESCs.

(A) Strategy for transgenic rescue experiment. CAG promoter derived Flag-tagged ECAT15-2 protein expressing vector based on piggyBac system was transducted into the 15-2KO ESCs

(B) Protein expression of ECAT15-1, ECAT15-2 and pluripotent markers Oct3/4. Note the exogenous ECAT15-2 was expressed extremely stronger than endogenous ones, thus the band of endogenous ECAT15-2 appeared very weak (arrow head).

(C) Relative mRNA expression of ECAT15-1, ECAT15-2 and several gametogenesis related genes. Error bar indicates the SD of three experiments.

(D) Two-dimensional scatter plots of log ratios of relative transcript levels by microarray analysis. Left panel indicated comparison between transcripts of wild-type and the mock transduced 15-2KO ESCs. Right panel indicated comparison between transcripts of wild-type and the Flag-ECAT15-2 transduced 15-2KO ESCs. Green bar indicated the borderline for 5 fold differences, and the blue dots indicated transcripts that were differentially expressed more than five folds between wild-type and the mock transfected 15-2KO ESCs. Note that the probe for ECAT15-2 (A_52_P16249) is designed on the junction of protein coding region and 3' UTR of ECAT15-2 mRNA sequence, and only the half of the probe (31bp) is able to hybridize to exogenous Flag-tagged ECAT15-2 mRNA. Therefore the exogenous Flag-tagged ECAT15-2 mRNA was not detected correctly.

Nakamura et al
Supplementary Figure 8

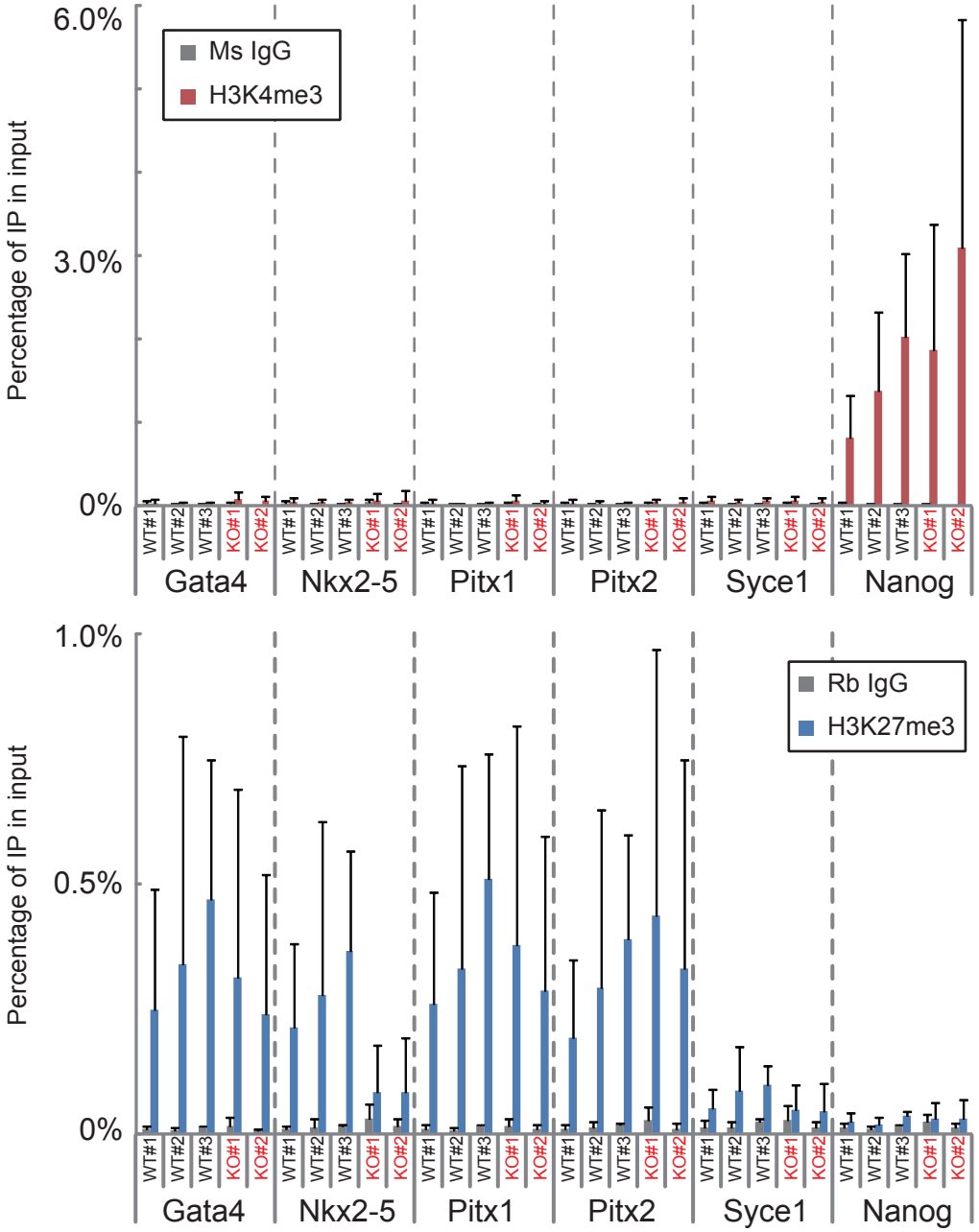

Supplementary Figure 8, Histone modification in the 15-2KO ESCs.
ChIP analysis using anti-H3K4me3 and anti-H3K27me3 antibodies. Precipitated DNA from wild-type ESC clones (WT) and the 15-2KO ESC clones (KO) were examined by quantitative PCR. Error bar indicates the SD of three experiments.

Supplementary table 1
Analysis of microarray data of the 15-2KO lung.

A. WT > 15-2KO　　84 entities

Probe ID	Gene Symbol	Fold change
A_51_P105380	2010005H15Rik	29.25
A_51_P438967	Gpnmb	14.14
A_52_P425734	Afm	12.98
A_52_P4201	Gata4	11.97
A_51_P444137	Syce1	11.51
A_52_P4724	AI851790	8.43
A_51_P361340	Nppa	7.97
A_51_P503756	Igl-V1	7.47
A_51_P110341	Scgb3a1	7.37
A_51_P277683	Ms4a1	7.10
A_51_P183051	Upb1	6.74
A_51_P196581	Olfr920	6.71
A_51_P310594	Aldh3a1	6.34
A_52_P779708	AK086756	6.32
A_51_P354126	Reg3g	6.09
A_52_P22324	Pln	5.94
A_51_P177210	Myl3	5.89
A_52_P456410	5330426P16Rik	5.77
A_52_P748350	TC1679528	5.61
A_51_P501897	Pitx2	5.57
A_52_P594116	Cyp21a1	5.45
A_51_P308912	Mybphl	5.09
A_52_P675599	Crb1	5.06
A_51_P485862	Eef1a2	4.99
A_52_P120803	Ankrd1	4.92
A_51_P264495	Pgam2	4.88
A_52_P48218	Tdrd1	4.82
A_51_P408116	Il1f9	4.70
A_51_P133684	Csrp3	4.69
A_51_P145132	Mcpt4	4.67
A_51_P249608	Trdn	4.64
A_51_P182244	Cdgap	4.60
A_51_P122071	Muc5b	4.57
A_51_P276267	Spib	4.50
A_51_P380807	Ckm	4.49

A_52_P386544	4930517K11Rik	4.48
A_51_P480190	Spaca1	4.36
A_51_P302327	Lgals7	4.28
A_51_P419439	Gnmt	4.27
A_52_P413395	Sln	4.24
A_51_P248638	Myoz2	4.06
A_51_P265348	Ldb3	4.01
A_51_P211506	Muc20	4.00
A_51_P416858	Myl1	3.85
A_51_P233855	Adprhl1	3.81
A_51_P173285	Nkx2-5	3.66
A_51_P465449	Mybpc3	3.57
A_51_P143855	Atg3	3.57
A_52_P349844	Obscn	3.55
A_51_P468558	Treml4	3.53
A_51_P435704	Tnni1	3.52
A_52_P256647	Fmn2	3.51
A_51_P275072	1110012N22Rik	3.48
A_51_P461894	Tnnc1	3.48
A_51_P413130	Myl4	3.46
A_51_P196695	Il7r	3.44
A_52_P423814	Cox8b	3.41
A_52_P51198	Slc35a5	3.40
A_51_P193185	Mb	3.37
A_52_P657360	Tnni1	3.37
A_51_P392459	Myl2	3.36
A_51_P421780	Myo18b	3.36
A_51_P119749	BY439412	3.30
A_52_P740427	EG624219	3.29
A_52_P298088	Itgb1bp2	3.24
A_52_P544523	Myl4	3.23
A_52_P517224	Trim63	3.04
A_51_P402160	Zfp750	3.01
A_51_P433989	Mapk10	2.99
A_51_P421300	Drd1ip	2.97
A_52_P184609	Gabrp	2.88
A_51_P247421	1700026J04Rik	2.88
A_51_P510418	Aldh1b1	2.84
A_51_P346445	Hspb7	2.76
A_51_P167292	Chi3l3	2.74
A_51_P164630	1110028A07Rik	2.73

A_52_P563123	Tnni3	2.71
A_51_P341725	Mesp1	2.68
A_51_P246345	Myl7	2.61
A_51_P447874	Hspb7	2.58
A_52_P362611	Ube2f	2.53
A_51_P108266	Actn2	2.50
A_51_P386983	Tnni3	2.49
A_51_P325173	Tpm1	2.44

WT < 15-2KO 22 entities

Probe ID	Gene Symbol	Fold change
A_52_P522255	Pitx1	76.86
A_52_P176026	Xlr4b	11.41
A_51_P457237	Xlr4b	10.66
A_52_P107956	AK048202	8.82
A_51_P513598	1700017N19Rik	8.53
A_51_P376127	Aire	6.71
A_52_P778709	AK047753	6.32
A_52_P90577	a (nonagouti)	6.10
A_51_P457244	Xlr4b	5.94
A_51_P280030	NAP057065-1	5.47
A_51_P204053	Hba-x	5.21
A_51_P358037	Abi3bp	4.80
A_52_P642736	TC1697128	4.63
A_52_P228833	Cdgap	4.55
A_52_P117771	EG209380	4.36
A_51_P322482	Pkhd1	4.17
A_52_P553408	D130060J10Rik	4.09
A_52_P691533	AK051672	3.75
A_51_P468770	4930455C21Rik	3.59
A_51_P399000	Hmbox1	2.96
A_51_P325651	Cd47	2.81
A_52_P276955	Epha3	2.27

The 106 entities were selected as two fold differentially expressed genes by comparison between wild-type lungs and the 15-2KO lungs. Genes listed in left panel indicate two fold down regulated genes in the 15-2KO lungs. On the other hand, genes listed in right panel indicate two fold up regulated genes in the 15-2KO lungs.

B.

Gene Ontology	Entities	P-value
contractile fiber	14	5.00E-30
contractile fiber part	12	3.10E-26
cytoskeleton	18	1.50E-20
myosin complex	7	2.40E-14
troponin complex	3	4.90E-13
muscle contraction	6	6.20E-13
heart development	8	4.40E-12
muscle organ development	7	2.60E-11
heart contraction	5	8.90E-11
blood circulation	6	1.40E-10
cytoskeletal protein binding	8	1.60E-10
actin binding	7	2.00E-10
regulation of muscle contraction	3	8.40E-10
regulation of heart contraction	4	3.70E-09
motor activity	5	6.10E-08
structural constituent of cytoskeleton	4	3.30E-07
cytoskeleton organization	7	4.30E-07
calcium ion binding	9	4.80E-07
cell differentiation	11	8.20E-06
heme binding	4	1.10E-05
tetrapyrrole binding	4	1.10E-05
heart morphogenesis	3	1.40E-05
cellular chemical homeostasis	3	2.30E-05
cellular ion homeostasis	3	2.30E-05
enzyme regulator activity	5	3.10E-05
muscle cell differentiation	3	5.90E-05
hemopoietic or lymphoid organ development	4	2.00E-04
blood vessel morphogenesis	3	2.00E-04
nucleoplasm	5	2.00E-04
anatomical structure formation involved in morphogenesis	3	2.00E-04
immune system development	4	2.00E-04
receptor binding	5	2.00E-04
cellular homeostasis	3	2.00E-04
vasculature development	3	3.00E-04
tube development	3	4.00E-04
embryonic development	5	5.00E-04
small protein conjugating enzyme activity	3	6.00E-04
carbohydrate binding	4	7.00E-04

transporter activity	7	1.20E-03
transport	10	1.30E-03
hemopoiesis	3	1.80E-03
carbohydrate metabolic process	4	1.80E-03
transcription	8	2.20E-03
transcription activator activity	3	2.60E-03
immune response	4	2.80E-03
sugar binding	3	2.80E-03
transcription factor binding	3	3.10E-03
response to stress	4	3.80E-03

The 106 entities from transcriptome analysis were analyzed by NextBio and top 30 terms that containing more than two genes are listed ($p<0.0001$).

Supplementary table 2, Primer List.

Primer & Probe	Sequence	length	discription
ECAT15-BAC-S2	AGATTCATTTACTTCACCGCTCCATCATAC	30	For screening PCR of ECAT15 BAC DNA.
ECAT15-BAC-AS2	TCCTGGTAATAAAATTCCGTCGCTGTTG	28	
15-1recomb5'-s	CCGCTCGAAGTGGCCTTGCGCGAGACCCTGGGGCCCGGGTGTAGATGTGTTGGCAGAACATATCCATCGC	70	For loxP-PGK-Neor-loxP fragment amplification into ECAT15-1 1st intron.
15-1recomb5'-as	AAATTCCTTCCTAACAAAGCATTCCTTCCAAAACACACCCTCCTCTCCTACTATCAACAGGTTGAACTGATGGC	74	
15-1Recomb3'-s	TTAGGGCAGAAGCTTTCTGTGAGATTGCTAGGCTTCTGTCTGTCCCAGTGTGGCAGAACATATCCATCGC	70	For loxP-PGK-Neor-loxP fragment amplification into about 1kbp downstream of ECAT15-1 locus.
15-1Recomb3'-as	GTGGAATATATGACATCAAATACAACCAGCAGTCGTCCATCAGGGGATGACTATCAACAGGTTGAACTGATGGC	74	
15-2-5'Recomb-s	CTGGGAGTAAAATGAAACTGTTTCCTTGCTAAAGGAGTAAATCGTCTCAGCCCTATGCTACTCCGTCGAAGTTC	74	For FRT-pgk-Hygr-FRT fragment amplification into ECAT15-2 1st intron.
15-2-5'Recomb-as	TTCAGCTCACCTTCTCGGTAGATTTTAATCCTAGCTTCAGCCTTCCTAGTCTGGCAGTTTATGGCGGGCGTCCT	74	
15-2recomb3'-s	AATACAGTGTATTTACCAGTGTACAGGCAGCTCACTCGCCTGCAGCTGAACCCTATGCTACTCCGTCGAAGTTC	74	For FRT-pgk-Hygr-FRT fragment amplification into about 1kbp downstream of ECAT15-2 locus.
15-2recomb3'-as	ACTACTGCCAGTTGATGACTGCTGGAGCACGGAGAGCCATCAGCAGTCAGCTGGCAGTTTATGGCGGGCGTCCT	74	
ECAT15-3'probe2-s	ACCCATAATAGCACCCATCTGTTA	24	For amplification of Southern blot probe for ECAT15 3' probe. Genomic DNA is used for template.
ECAT15-3'probe2-as	TTGCCTAATTTCTTTTTCTCAATAC	25	
hygro-S78	CGACAGCGTCTCCGACCTGATGCAGCTC	28	For amplification of Southern blot probe for Hygromycin registant gene probe. Inserted cassete is used for template
hygro-AS992	GGGCGTCGGTTTCCACTATCGGCGAGTA	28	
Q15-1-s2	AGAAGAGAAGAATGAGCGTTACAAT	25	Primers and Taqman probe for genomic qPCR of ECAT15-1 locus
Q15-1-as2	GGATTCTAAATTCCTTCCTAACAAA	25	
15-1Taq (Taqman Probe)	CGGGTGTAGATGTGTTAGGAGAGGA	25	
Q15-2-s	ATGAATACAGTGTATTTACCAGTGT	25	Primers and Taqman probe for genomic qPCR of ECAT15-2 locus
Q15-2-as	GAGCTACTACTGCCAGTTGATGACT	25	
15-2Taq(Taqman Probe)	CCTGCAGCTGAACTGACTGCTG	22	

Qnanog-s	GTCCTTAGAAGTTGCTGTAATGTAA	25	Primers and Taqman probe for genomic qPCR of Nanog locus
Qnanog-as	TCACATAATTATGATTTTAACAGGC	25	
NanogTaq(Taqman Probe)	TGAATCGAACTAACGTCTGGACGTC	25	
15-1G-s1	ACAACAGGAAGTAGGAGGAGATTTT	25	Genotyping primer set among ECAT15-1 WT, CT and KO allele detection
15-1G-as1+	GAAGTGACAATTTAGCATTTCCTGT	25	
15-1G-as1-	GAGCTCAGACCATAACTTCGTATAA	25	
15-2G-s1	TGAGACCCAGAGAACTGATAAAATC	25	Genotyping primer set between ECAT15-2 WT and KO allele detection
15-2G-as1+	TTTGTATAGCGCCTTATCAAAGTTC	25	
15-2G-as1-	GAGCGGAAGTTCCTATACTTTCTAG	25	
Q15-1-s2	AGAAGAGAAGAATGAGCGTTACAAT	25	Genotyping primer set between ECAT15-1 WT and Flox allele detection
15-1-Reds5'-as	AGATTCTGAGGGCCTATGGATAAA	24	
15-2Reds	GCACAGGCTGGTCTTGAGTATTTT	24	Genotyping primer set between ECAT15-2 WT and FRT allele or between WT and CT allele detection
15-2reds3'-as	AGACAAGCCCGAGACACATCCGTC	24	
PGK-ASseq	ACCGGTGGATGTGGAATGTG	20	
15-2_5'->EGFP	GCATTCATTCAGCGGCTGCCTTTGTCTTCTTCCAAGCCTGCCTGAAAATGATGGTGAGCAAGGGCGAGGAGCTGTTCA	78	For EGFP-FRT-pgk-Hygr-FRT fragment amplification into ECAT15-2 start codon.
15-2_3'->PHF	TAGAGAATCAATTCTCTTACCTCGTTGAAAGTCTCCAGGCCGAAGTATGAATAGGGCGAATTGGAGCTCCACCGC	75	
EGFP-UP	CGACTTCTTCAAGTCCGCCATGCCCG	26	Genotyping primer set for inserted EGFP gene
EGFP-LOW	CCAGCAGGACCATGTGATCGCGCTTC	26	
15-1-ISHprobeA-s	GCTGGCGTCACTCACTCTTG	20	For amplification of in situ hybridization probe for ECAT15-1 probe. ECAT15-1 cDNA is used for template.
15-1-ISHprobeA-as	ACAACACACTACAACCCAGG	20	

15-1qPCR-s1	AGTCAACCTAGCACGGCTC	19	Detection for ECAT15-1 mRNA by Real-Time RT-PCR.
15-1qPCR-as1	TCCTGGCGTCTCAGTGTCT	19	
15-2qPCR-s2	ACACAGACTACGCTACGCAAT	21	Detection for ECAT15-2 mRNA by Real-Time RT-PCR.
15-2qPCR-as2	GTTGGGTGTTTGATTCCAGCA	21	
NAT1U283	ATTCTTCGTTGTCAAGCCGCCAAAGTGGAG	30	Detection for Nat1 mRNA by Real-Time RT-PCR.
NAT1L476	AGTTGTTTGCTGCGGAGTTGTCATCTCGTC	30	
SP-C_RT_s205	CTCCACATGAGTCAAAAACATACTG	25	Detection for SP-C mRNA by Real-Time RT-PCR.
SP-C_RT_as607	AGTAGAGTGGTAGCTCTCCACACAG	25	
Scgb1a1-RT-s21	ACAATCACTGTGGTCATGCTGT	22	Detection for Scgb1a1 mRNA by Real-Time RT-PCR.
Scgb1a1-RT-as291	ATCTTGCTTACACAGAGGACTTGTT	25	
Gata4-RT-S	TCGACAGCCCAGTCCTGCACAG	22	Detection for Gata4 mRNA by Real-Time RT-PCR.
Gata4-RT-AS	GCTTAATGAGGGGCCGGTTGAT	22	
mGata6-qPCR-s2	CTGTGCAATGCATGCGGTCTCTACA	25	Detection for Gata6 mRNA by Real-Time RT-PCR.
mGata6-qPCR-as2	CACACAGGCTCACCCTCAGCATTTC	25	
mNkx2.5-qPCR-s	CATTTTACCCGGGAGCCTACGGTGA	25	Detection for Nkx2-5 mRNA by Real-Time RT-PCR.
mNkx2.5-qPCR-as	CTTTGTCCAGCTCCACTGCCTTCTG	25	
mPitx1-qPCR-s	ATGAGCATGAGAGAGGAGATCGCGG	25	Detection for Pitx1 mRNA by Real-Time RT-PCR.
mPitx1-qPCR-as	CTTGCACAGGTCCAACTGCTGGTTC	25	
mPitx2total-qPCR-s	AAACCGCTACCCAGACATGTCCACT	25	Detection for total Pitx2 mRNA by Real-Time RT-PCR.
mPitx2total-qPCR-as	GTTGCGTTCCCGCTTTCTCCATTTG	25	

mDdx4(Mvh)-qPCR-s1	TGGGAGATGAAGATTGGGAGGCAGAA	26	Detection for total Ddx4(Mvh) mRNA by Real-Time RT-PCR.
mDdx4(Mvh)-qPCR-as1	AGACTCGCCAATATCTGATGAAGCTGA	27	
mMael-qPCR-s1	CTCATTGTGAACAGCGCTTCCTCCC	25	Detection for total Mael mRNA by Real-Time RT-PCR.
mMael-qPCR-as1	AGAATCACTTGCAGCCTGGCAATGG	25	
mSyce1-qPCR-s1	AACGGCAGAGGCTGAAGGAAGAACT	25	Detection for total Syce1 mRNA by Real-Time RT-PCR.
mSyce1-qPCR-as1	GGCCATCCTCCATGAGCTGTCTTCT	25	
me-mGata4-F2	GGGGTAATAGTAATAGTAATTTGTAGTTAG	30	Primer set for Bisulfate sequencing analysis of Gata4 promoter locus.
me-mGata4-R2	ACCTTAAAACCCATTCAAAAACTATAATT	29	
meNkx2-5-F4	GGTTGTTTTTAGGGGTGGGTAG	22	Primer set for Bisulfate sequencing analysis of Nkx2-5 promoter locus.
meNkx2-5-R3	ACTTAAAATTCTCCTTACCTTTTTTATCC	29	
mePitx1-F3	GTTTTAGGGGAGAGGGTTTAAATTAATTAG	30	Primer set for Bisulfate sequencing analysis of Pitx1 promoter locus.
mePitx1-R5	CAACTCCTATCTAAACCACCTCAAATC	27	
me-mPitx2-F1	TTGAATTTTGAAAGTGGGGAAAGAGT	27	Primer set for Bisulfate sequencing analysis of Pitx2 promoter locus.
me-mPitx2-R1	CTACATTTTAAACCATCTCTAACCTTATA	30	
meSyce1-F1	GTGGTGGGGGTATGGTTTTA	20	Primer set for Bisulfate sequencing analysis of Syce1 promoter locus.
meSyce1-R1	ATCCCAATCAACCCTCTCC	19	
mGata4-ChIP-s2	CAGGTGGTATTCCAGCCCTCTCCTG	25	Primer set for ChIP-qPCR analysis of Gata4 promoter locus.
mGata4-ChIP-as2	TCACAGGGCCCTATTACCGCGTAAA	25	
mNanog-ChIP-s1	GCTGCGGCTCACTTCCTTCTGACTT	25	Primer set for ChIP-qPCR analysis of Nanog promoter locus.
mNanog-ChIP-as1	AGTGTGATGGCGAGGGAAGGGATTT	25	

mNkx2-5-ChIP-s1	CACCACTCTCTGCTACCCACCTGG	24	Primer set for ChIP-qPCR analysis of Nkx2-5 promoter locus.
mNkx2-5-ChIP-as1	GCTGCTGCTCCAGGTTCAGGATGTC	25	
mPitx1-ChIP-s4	AGCCCAGGGTTGTGAGACATCAGTC	25	Primer set for ChIP-qPCR analysis of Pitx1 promoter locus.
mPitx1-ChIP-as4	TCCACATCCCCCTTTGTTTTGCACC	25	
mPitx2iso1,2-ChIP-s3	TGGGGAAAGAGTTGTCTGGGCAGAT	25	Primer set for ChIP-qPCR analysis of Pitx2 promoter locus.
mPitx2iso1,2-ChIP-as3	ATCAGTCTGGCCAGGAGCTGGTG	23	
mSyce1-ChIP-s1	TATTTGGTGGTAGTGGTGGTGGGGG	25	Primer set for ChIP-qPCR analysis of Syce1 promoter locus.
mSyce1-ChIP-as1	TCTGGTGGCCATACTGCTCCACTTC	25	
IAP +4.3 ChIP F	AAGCAGCAATCACCCACTTTGG	22	Primer set for ChIP-qPCR analysis of IAP locus.
IAP +4.3 ChIP T/C R	CAATCATTAGATGT/CGGCTGCCAAG	24	